Novel Tools for Research and Education in Seismology

by

Mikhail E. Boulaenko, B.Sc.

Master of Science Thesis

Institute of Solid Earth Physics, University of Bergen

Allégaten 41, 5007 Bergen, Norway

December, 2002

Thesis summary

It's first part describes the noise performances of an inexpensive instrument for seismic data collection; the geophone-based seismograph used in the SEIS-SCHOOL network and now called Cossac Ranger. The analysis of its properties such as the transfer function and the thermal stability is given. A theoretical model for the instrumental noise calculation is proposed and then the instrumental noise RMS spectral density curves are calculated. Based on the obtained noise level it is concluded that the performance of the geophone-based seismograph is comparable to that of a standard short period seismometer. Further, it was found that the instrumental noise at frequencies below $10Hz$ is mainly generated by the operational amplifier circuits.

According to the above analysis three alternative preamplifier design solutions were proposed and analyzed. One of them showed better noise performances then those of the original design. The new design also forwards a simplification of the assembling process of the preamplifier. In Appendix A a set of equations for a geophone transfer function and impedance is developed. Appendix B presents theory of operation of the over-damping preamplifier. A theoretical model for calculation of the instrumental noise of the preamplifier is highlighted in Appendix C.

The second part of the thesis is devoted to electronic learning technologies. It highlights the conceptual design of the SEIS-SCHOOL project e-learning modules and gives a brief description of its practical application. It starts with an overview of available Web-technologies for creation of advanced electronic learning modules. Then demonstrates that such technologies and freeware suffice for creation of such modules. Important here is that costly commercial software is not needed for compliance to high-level e-learning standards regarding modules accessibility, durability, interoperability, and content reusability.

The third part describes the content of the e-modules being created for high school students, as well as a description of the first of these e-modules. An overview of the basic design principles is given. The software package for the interactive seismicity

mapping and statistical catalog analysis “SEISMOTECTONICS” used as a practical task in the e-learning framework is also presented.

Acknowledgments

I would like to express my largest gratitude to my supervisor, Professor Eystein S. Husebye for his never ending enthusiasm and guidance during this work. He is the one who inspired my leap from Quantum Electronics to Seismology which would be impossible without his well-know scientific attitude. Also I would like to acknowledge Dr. Yuri Fedorenko for his insightful introduction to over-damping preamplifiers and great support during my studies.

The work on electronic learning has been done with the strong collaboration of the STATOIL sponsored E-modulprosjektet leaded by Professor Jonny Hesthammer at the University of Bergen and Dr. Thor A. Thorsen at the University of Oslo whom I would like to express my gratitude for their brilliant guidance on e-learning. I would like to thank students who were working with me during Statoil’s Sommerprosjektet 2002 for the inspirational atmosphere and their positive attitude.

This work have been done at the Institute of Solid Earth Physics of the University of Bergen which students and employees I would like to acknowledge for the help during my studies. I am grateful to the teaching staff at the institute which provided me a strong basis in geosciences.

Contents

I Noise performances of the geophone-based seismograph 1

1 Introduction 3

2 Design 6

2.1 Geophones as seismometers 8

2.2 Over-damping technique for flattening of the geophone response 9

2.3 Preamplifier design 17

3 Instrumental noise 20

3.1 Suspension noise of the geophone proof mass 23

3.2 Johnson's or thermal noise of the electronic dissipative components 25

3.3 Noise of the active electronic components 27

3.4 Results 28

4 Preamplifier design improvement 31

4.1 Two versus single cascade preamplifier design 31

4.2 Operational amplifiers performance: JFET versus BIPOLAR 33

4.3 Optimal preamplifier design for the GS-11D $4k\Omega$ geophone 35

4.4 Influence of the geophone coil resistance 35

4.5 Conclusions 37

5 Inverse-filter technique for flattening of the geophone response 42

5.1 Inverse-filtering preamplifier design 44
5.2 Numerical simulation results 44
5.3 Current step-release calibration technique 45
5.4 Conclusions 45

6 Conclusion and discussion **47**

II Advanced e-learning modules for high schools: applying modern Web-technologies **51**

7 Introduction **53**

8 SCORM standard for Web-based e-learning **55**
8.1 SCORM Content Aggregation Model 56
8.2 SCORM Content Model 57

9 XML the Web-based standard for content storage and exchange **59**
9.1 SVG the Web-based delivery format 60

10 SEIS-SCHOOL e-module conceptual model **61**
10.1 SEIS-SCHOOL e-module creation process 63
10.2 Creating SVG animations 65

11 Conclusions **67**

III Electronic learning modules for high school students in seismology **70**

12 Introduction **72**
12.1 “The Dynamic Earth” 73
12.2 “The Kinematic Earth - Its Scandinavian manifestations” 75
12.3 Interactive seismogram analysis module 75

13 General modules features **77**

13.1 Design principles 78

13.2 Content 78

13.3 Presentation format 79

13.4 Automated production process 80

13.5 Learner's evaluation 82

13.6 Practical tasks - interactive tools for statistical seismic catalog analysis . 83

14 Conclusions **86**

IV Appendixes **89**

A Geophone theory **90**

A.1 Geophone transfer function 90

A.2 Geophone impedance 94

A.3 Summary 95

B Theory of operation of the over-damping preamplifier **97**

B.1 Design 97

B.2 Transfer function 98

B.3 Input resistance 99

B.4 Feedback resistors 99

B.5 Summary 100

C Instrumental noise model for the over-damping preamplifier **101**

C.1 Preamplifier circuit equivalent noise 101

C.2 Thermal noise of the feedback resistors 102

C.3 Thermal noise of the geophone coil 104

C.4 Noise of the operational amplifiers 104

C.5 Summary 106

Part I

Noise performances of the geophone-based seismograph

Noise performances of the geophone-based seismograph

by

Mikhail E. Boulaenko and Eystein S. Husebye

Institute of Solid Earth Physics, University of Bergen

Allégaten 41, 5007 Bergen, Norway

December, 2002

Chapter 1

Introduction

Our abilities to map and understand the dynamics of the Earth are closely coupled to access of high quality earthquake recordings from local, regional and global seismograph networks. The high costs of modern stations and besides also high operational costs limit the number of stations in operation. These factors also pose a limitation to educational projects as an incentive for fostering science interest among high school students because operating their own seismograph station is strongly motivating. To buy stations at commercial price of $10000 is naturally out of question for educational projects while the alternative of accessing professional data bases is not a good substitute. The challenge here, and in reality a prerequisite for educational projects, is to build inexpensive seismograph stations of high quality.

Several attempts have been launched in countries like Australia, New Zealand, USA but most of these projects have not been successful. Major drawbacks have been either poor quality of the seismic stations, clumsy data access and/or lack of signal analysis software. Particularly major efforts have been done in United States by the Princeton Earth Physics Project (PEPP) which was lunched in 1994 and involves high schools through out the whole country. PEPP has been initiated and coordinated by Prof. Guust Nolet (University of Princeton), and related documentation is (http://lasker.princeton.edu/). Presently, the PEPP network consists of 70 seismic stations. In Europe major efforts

are the The Educational Seismological Project (EduSeis) which involves local school station networks in Italy, France, Germany, and Portugal. Project information is available in Internet (http://www.eduseis.org). A major drawback with the above efforts is that easy access to own seismograph recordings are seldom available. Either data are extracted from remote stations at an anonymous data base or even if 'own' record access is feasible data handling and analysis is far to complicated and awkward. Simply, to watch in terms of high school students data must be available in near real time and display and analysis must be feasible in Internet.

In 2000 Professor Eystein Husebye, and Researcher Yuri Fedorenko launched the SEIS-SCHOOL project which goals are promotion of earth sciences and especially seismology among high school students and also providing quality seismic data for scientific research. A critical project aspect was to design and build seismograph stations which could be deployed in the school yards of the participating high schools. An implicitly, major goal of our seismic network is monitoring of local seismicity which requires high quality of the seismic data collected and well-developed educational standard data analysis software. Currently the SEIS-SCHOOL network consists of 6 seismic stations installed in high schools and permanently connected via Internet to Hub at the Institute of Solid Earth Physics.

I was involved in the initial part of the project tied to the development of the seismic stations software and hardware. During the seismograph station design many innovative solutions have been applied. The major one is the geophone as a substitute for the costly seismometer. In order to make its frequency response equivalent to the response of the short period seismometer the 'over-damping' preamplifier have been applied. This preamplifier was firstly proposed by Lippmann et al. (1983) and actually used by Fedorenko et al. (1999) in their Cossac Ranger design. Complete study of the noise performance for such a preamplifier was not available before. The aim of this work is to undertake complex theoretical noise analysis, and forward some possible design solutions for the noise level optimization. In Chapter 2 the general seismograph description, as well as the preamplifier operation theory and analysis are given. In Chap-

ter 3 the theoretical calculation of the instrumental noise spectra for the seismograph is performed. Some design improvements which can be applied in order to decrease the noise level are proposed in Chapter 4. An overview of an alternative preamplifier design based on the inverse-filtering technique is given in Chapter 5 together with its comparative analysis with the over-damping technique.

Chapter 2

Design

In practice, a seismometer, a pendulum device, has to be complemented with a preamplifier, filtering device, clock for accurate and absolute timing plus an analog-digital converter for proper data recording in digital form. With all these extras the seismic measuring device is denoted a seismograph station. Up to the 1960-ties most seismograph stations in operation were mechanical with low amplification and hence low sensitivity. In the extreme the pendulum mass exceeded 10 tonnes in weight. However, with steady progresses in instrumentation engineering, and extensive use of electronics a modern seismograph station just weight a few kilos and are able to record ground motion down to the nanometer level over a wide frequency range say 0.005 - 50Hz. These advanced designs are very expensive with a price tag around $50000 for just one station. Even modest station designs used for monitoring local EQ activity using short period seismometers only, are not cheap with prices around $10000 for just one unit. The most recent developments are tied to deploying seismographs on planet Mars - these instruments now under development are not cheap either.

The first requirement to "educational seismic networks" is a low station price, which makes schools able to afford it. Usually the major part in the cost of the seismograph station is seismometer. For example a cheap short period instrument costs about $2500, so for 3-component recording net cost is $7500. In the SEIS-SCHOOL network an inex-

pensive 3-component seismograph developed by Yuri Fedorenko and colleagues is used (Fedorenko et al., 2000). The significant price lowering is foremost obtained by replacing costly seismometers with inexpensive geophones at $60 each. Quality is ensured by the newly constructed preamplifiers and A/D converters. Finally our station net cost is about $1000 (parts only), while records are of high quality which will be demonstrated in this thesis. Note SEIS-SCHOOL stations are installed in school yards, while ordinary professional stations usually located in non-populated areas which presumably are characterized by low cultural noise levels. For monitoring small seismic events at regional and teleseismic ranges a low noise level operational environment is important. However, for local events the distance to source is far more important due to fast signal amplitude decay. In a scientific context, research is always tied to event recordings with good-to-excellent signal-to-noise ratios (SNR). In the SEIS-SCHOOL network, it is essential with the free Internet connections as offered by school yard installation and not optimum station sites is not much of a problem in a local event monitoring context.

The permanent Internet connection allows us to run the seismic station timing using Internet Network Time Protocol (NTP) originally developed by Professor David L. Mills at the University of Delaware. The NTP is an Internet protocol used to synchronize the clocks of computers to some time reference with sufficient precision for seismological applications. The important problem is how to synchronize computer clock, or any other time source such as GPS or radio clock, with the over-sampling frequency generator of the A/D converter. This is a major problem for all old style A/D converters, because their sampling frequency is strongly defined by hardware, and it is usually synchronized directly to the GPS receiver. So-called "double clock", systems lack even this synchronization, thus avoiding all synchronization problems, but causing significant problems with data processing. In our station design this problem doesn't appear because the ADC sampling process is fully implemented in the station software. Here we use the ability of the real-time operational system (RT-Linux) for extremely precise timing, making any hardware frequency generators unnecessary. This solution was developed by me in the first steps of the station design, and gives us very high level

of flexibility and control in the station timing and A/D converter oversampling process. Thus our stations can be synchronized by GPS, radio clock, or NTP. The excessive oversampling allows us to provide real 19 bit resolution data, while using relatively cheap 16 bit high oversampling linear A/D converter designed by Evgeny V. Boulaenko, St. Petersburg. The use of the NTP allows us to avoid a GPS receiver installation, in sites with the permanent Internet access, hence decreasing station net cost by approximately $300.

2.1 Geophones as seismometers

A seismograph station aims at monitoring earthquakes activity and most important to provide data for research. The latter task entails that the seismic recordings reflect the true ground motion excited by a seismic source. In practice this implies that seismographs should be high quality instruments which require a stable and stationary operational environment. In seismic profiling geophones are much used for subsurface imaging of geological strata but their operational environment is seldom stable nor stationary. In other words, the seismic field sensor that is a simplified pendulum device popularly called geophone, has a rugged design and is easy to deploy in the field. The most striking contrast to seismometers is in size and cost which is of the order of $60 per unit versus seismometer costs of $2500 or more. Understandingly, over the last 50 years there has been many attempts to modify geophones to work like a seismograph the rational being that the differences in wave field recordings are less striking than cost differences will imply.

There are several different geophones available on the market today. Some of them have low resonant frequency (down to 1 Hz), big proof mass (about 0.5 kg), high sensitivity (up to 3000V/$\frac{m}{s}$) and quite high price, at $500. The cheapest sensors cost about $10 and have high resonant frequency (10-100 Hz), low proof mass and correspondingly low sensitivity. In this context, the GS-11D 4.5 Hz Geospace geophone, appears to be an optimal choice for a short period seismograph. This geophone is widely used

Parameter	Symbol	Value	Tolerance, %	Units
Resonant frequency	f_0	4.5	17	Hz
Coil mass	m	0.024	5	kg
Damper constant	D	0.45	20	$N/(m/s)$
Spring constant	K	18.86	20	N/m
Generator constant	G	104.9	10	$V/(m/s)$
Normalized transduction const.	K_g	1.6586	10	$V \cdot s/(m \cdot \sqrt{\Omega})$
Coil resistance, $T = 25^oC$	R_{coil}	4000	5	Ω
Coil thermal constant	α_g	0.0034	-	$1/^\circ C$
Coil inductance	L_c	50	-	mH
Coil parasitic capacitance	C_c	50	-	pF
Total harmonic distortion	THD	0.2	-	%
Case to coil motion	z	1.8	-	mm
Mechanical damping	h_m	0.34	-	-

Table 2.1: Physical characteristics of the Geospace GS-11D 4.5Hz geophone used in the SEIS-SCHOOL seismograph. The values are taken from the factory specifications and Barzilai et al. (1998).

in field instrumentation for seismic surveys. It has a constant sensitivity to ground velocity (about 600V/$\frac{m}{s}$) for the frequency 4.5 Hz and higher. It is cheap (about $60) and could easily be transformed to a short period seismometer with flat response to acceleration in the frequency band from $0.25Hz$ to $90Hz$. Some key parameters for this geophone are given in Table 2.1. This geophone model is now being used in the SEIS-SCHOOL seismograph network, its characteristics are summarized in Table 2.1.

2.2 Over-damping technique for flattening of the geophone response

A geophone is essentially an electromagnetic velocity transducer. It measures ground acceleration and its output is proportional to the velocity of its proof mass. All mechanical end electrical parameters are factory defined and can not be changed without mechanical modifications. Attempts to make such modifications were made by Barzilai (1998) in order to improve the performance of this geophone through capacitive position sensing and feedback.

The only one parameter which can be changed by external electronic components is the damping of the mass-spring system, which affects the geophone response as detailed in Appendix A.1. Figure. 2.1 shows different response curves for the GS-11D 4.5Hz geophone for varying damping factor h. The seismograph response (Appendix A the equation A.6) to the ground acceleration is:

$$H(\omega) = \frac{V_{out}(\omega)}{\ddot{x}} = \frac{-i\omega G}{\omega^2 - \omega_0^2 + 2ih\omega\omega_0} \tag{2.1}$$

where ω - angular frequency, ω_0 - resonant angular frequency of the geophone, G - generator constant, h - damping factor, $\ddot{x}$ - ground acceleration, V_{out} - geophone voltage output. A typical damping factor used in geophysical applications is $h = 0.7$. As we see in the figure the response of the geophone to the ground acceleration for this damping factor has a narrow peak of high sensitivity at the resonant frequency of $4.5Hz$. Its roll-off is proportional to frequency ω. Increasing damping the response becomes less 'peaked' around the resonant frequency, while sensitivity in the flat bandwidth decreases. A solution here is to apply a high damping, say $h = 10$, to achieve a flat acceleration response in $0.25 - 90Hz$ band, and increase the sensitivity by introducing high gain in the preamplifier.

In Appendix A, equation (A.5) gives the damping factor of an electromagnetic seismometer connected to a preamplifier in the form:

$$h = \frac{1}{2\sqrt{mK}} \left(D + \frac{G^2}{R_{coil} + R_{preamp}} \right) \tag{2.2}$$

where R_{preamp} - input resistance of the preamplifier, while the other parameters are the geophone physical characteristics defined in Table 2.1. In order to increase damping it is necessary to decrease the input preamplifier resistance. The maximum damping feasible using so-called 'inverting' preamplifier with input resistance R_{preamp} set to zero is limited by the geophone coil resistance. For the GS-11D geophone the maximal damping is equal to $h = 2.4$ (Figure 2.2). From equation (2.2), for a predefined damping factor equal to 10, the preamplifier input resistance must be:

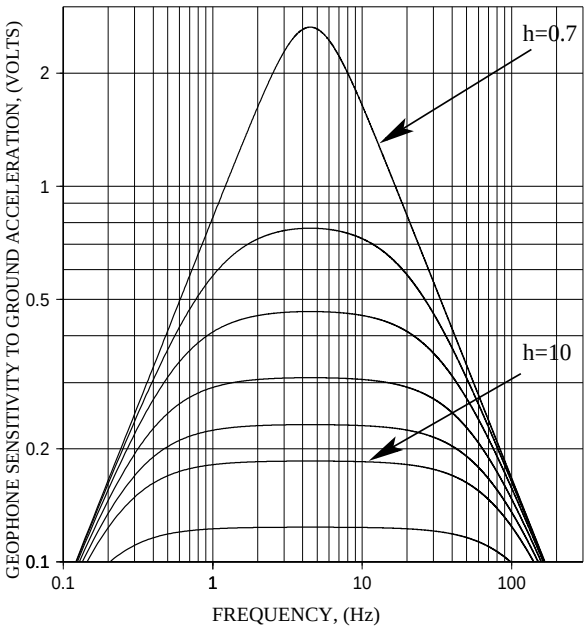

Figure 2.1: Sensitivity to ground acceleration $V/(m/s^2)$ curves for the GS-11D geophone, versus frequency Hz. The curves are calculated using equation 2.1 for different damping factors of 0.7,2.4,4,6,8,10 and 15 respectively.

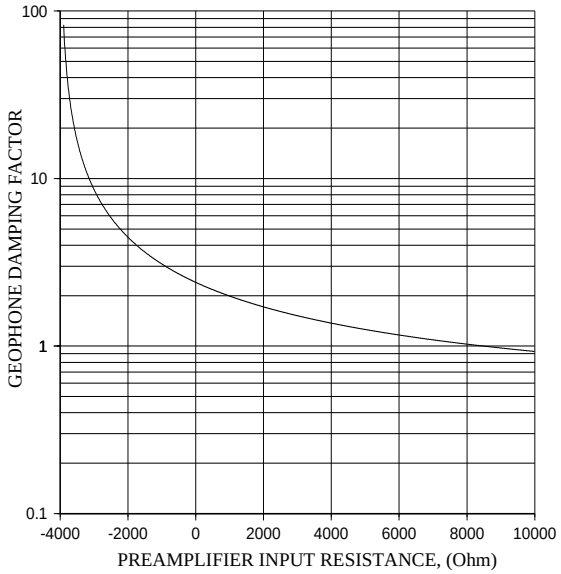

Figure 2.2: Damping factor h versus the preamplifier input resistance $Ohms$, calculated using the equation (2.2) for the GS-11D geophone with the coil resistance $R_{coil} = 4000\Omega$. The damping increases inverse proportionally to the input resistance. When the preamplifier input resistance is equal to zero the damping is equal to $h = 2.4$. In order to achieve a damping factor more when $h = 2.4$ the input resistance must go negative.

$$R_{preamp,h=10} = \frac{G^2}{2h\sqrt{mK} - D} - R_{coil} = -3146.43$$

In other words, to achieve a damping factor of 10 it is necessary to use a preamplifier which has negative input resistance. The method of flattening E-M seismometer responses using negative input resistance preamplifier was suggested by Lippmann et al. (1983) and later used by Fedorenko et al. (1999).

One of the disadvantages of this approach is the strong dependence of the preamplifier gain and the damping factor on changes in the geophone coil resistance, which is temperature dependent. The coil dependence on temperature can be expressed as a linear approximation using the standard formula for metallic conductors:

$$R_{coil}(T) = R_{coil0}\left(1 + (T - T_0)\,\alpha_g\right) \tag{2.3}$$

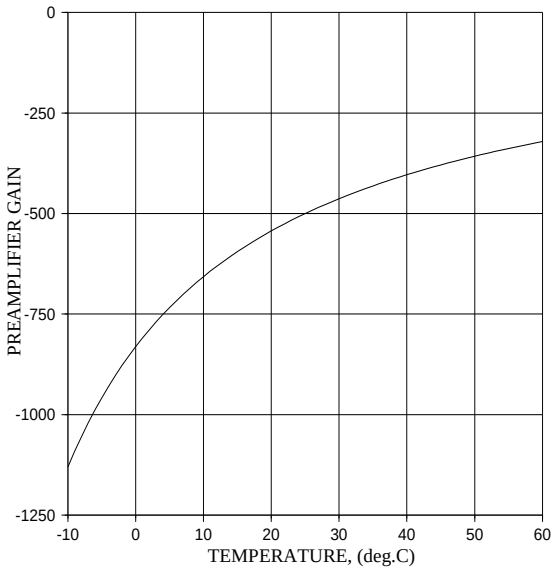

Figure 2.3: Preamplifier gain in the bandwidth versus the coil temperature, calculated using the equation 2.5 for the preamplifier designed to achieve a gain equal to -500 when the coil has temperature $25°C$. In the operation temperature range from $-10°C$ to $60°C$ the deviation is approximately $\pm 50\%$.

where T is the absolute temperature in $Kelvins$, R_{coil0} is the coil resistance at the temperature T_0, and α_g - is the geophone thermal constant. For the GS-11D geophone $\alpha_g = 0.34\%/°C$ (Fedorenko et al., 1999). According to Appendix B the equation (B.3) gives the preamplifier gain as:

$$A = \frac{\gamma_p + 1}{\gamma_p - \gamma_n}$$

where $\gamma_p = \frac{R_1}{R_2}$ and $\gamma_n = \frac{R_c}{R_3}$, with $R_c = R_{coil}/2$, are the positive and negative feedback parameters, described in Appendix B. Now consider the coil resistance being temperature depended, then the negative feedback factor also becomes temperature depended:

$$\gamma_n(T) = \frac{R_{coil}(T)}{2R_3} \tag{2.4}$$

and so the preamplifier gain becomes:

$$A(T) = \frac{\gamma_p + 1}{\gamma_p - \frac{R_{coil}(T)}{2R_3}} \tag{2.5}$$

Figure 2.3 shows the preamplifier gain versus temperature, calculated using the equation (2.5). The operational temperature range is approximately $\pm 50\%$, the preamplifier is designed to provide the amplification $A = -500$ at the temperature of $+25°C$

The damping factor of the geophone is defined by the preamplifier input resistance, from Appendix B, it is equal to:

$$R_{preamp} = 2R_3(\gamma_n - \gamma_p) - R_{coil}$$

In its temperature depended form:

$$R_{preamp}(T) = 2R_3(\gamma_n(T) - \gamma_p) - R_{coil}(T)$$

Finally the equation for the damping factor (2.2) as a function of temperature becomes:

$$h(T) = \frac{1}{2\sqrt{mk}} \left(D + \frac{G^2}{2R_3(\gamma_n(T) - \gamma_p)} \right) \tag{2.6}$$

In Figure 2.4 the geophone damping versus ambient temperature, is shown for $R_{preamp} = -3146\Omega$. The preamplifier is designed to provide damping $h = 10$ at temperature $+25°C$.

In Figure 2.5 the seismograph transfer functions are shown for different ambient temperatures, calculated using the equations (2.6),(2.4) and (2.1). The seismograph is designed to provide $90Hz$ bandwidth at $+25°C$, but as shown above it is temperature dependent. When, for example, the ambient temperature rises up to $+60°C$ the bandwidth narrows down to $60Hz$. And when the temperature decrease to $-10°C$ it widens to $110Hz$. The gain, within the bandwidth range, varies by 5% of the given level, and its value decreases when temperature increases. To summerize; when the temperature

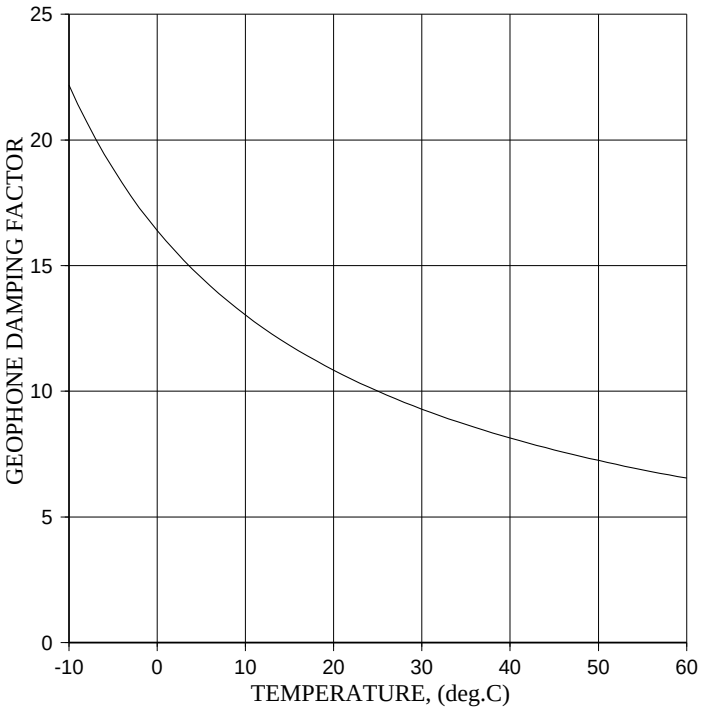

Figure 2.4: Damping versus the coil temperature, calculated using the equation (2.6) for the GS-11D geophone. The preamplifier was designed with the damping factor equal to 10 at $25°C$

increases preamplifier gain decreases, but at the same time the decrease in the geophone damping increase its sensitivity so the net seismograph gain variations remain small.

In climates with large temperature fluctuations we may want to safe guard against temperature gain variations. There are two options for solving this problem; the first is to install seismometer in a thermostable environment (e.g inside the buildings, boreholes, etc.) in order to decrease bandwidth variations. The second one is to use a preamplifier which update it's input resistance according to ambient temperature in order to keep the given gain and damping factor stable. The last method was suggested by Fedorenko et al. (2000).

If the case when exact bandwidth is not vital for desired application other method can be used. Such as adding a simple gain correction module in the preamplifier de-

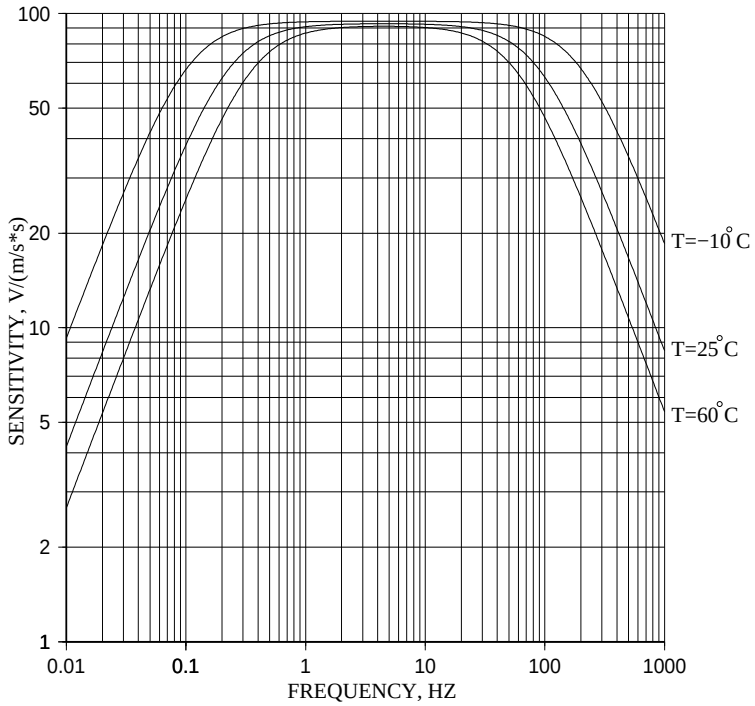

Figure 2.5: Curves for the seismograph sensitivity to ground acceleration at different ambient temperatures, versus frequency. Calculated using the equations (2.6) and (2.1) for the GS-11D geophone. The preamplifier is designed to provide $90Hz$ bandwidth at $+25°C$.

sign, stabilizing only the seismograph response within the given frequency band. And take the worst case of possible bandwidth as an effective seismograph bandwidth. Or if $\pm 2.5\%$ gain error is acceptable - no correction is required, when the seismograph parameters could be taken as an average gain and the narrowest bandwidth on the resonant frequency in the defined operating temperature range.

2.3 Preamplifier design

In this section a brief presentation of the preamplifier electrical design is given. Early designs of preamplifiers for electromagnetic seismometers were based on a suit of discrete analog elements. Nowadays, the types in use are mainly so-called "inverting" and "non-inverting" preamplifiers, based on operational amplifiers integrated circuits. Basic theory of their operation is given by Horowitz et al. (1990) among others. Riedesel et al. (1990) and Rodgers (1992) give analysis of noise parameters of these preamplifiers when applied to various seismometers.

The preamplifier design of the SEIS-SCHOOL seismograph is given in Fedorenko et al. (2001) and shown in Figure 2.6. This preamplifier has a differential voltage output for effective signal transmission to the A/D converter board. The design is based on industrial standard low noise bipolar input operational amplifiers OP27. The input resistance of the preamplifier is negative and equal to $R_{preamp} = -3146\Omega$. The theory of the operation of the negative input resistance preamplifier is given in Appendix B. The parameters of the SEIS-SCHOOL preamplifier are set to provide a geophone damping equal to $h = 10$, and signal amplification $A = -500$. The signal amplification must ensure a minimum ground acceleration to be recorded at adequate A/D converter (ADC) resolution. The latter is $R_{ADC} = \frac{\mathrm{U_{ADCmax}}}{2^{N_{bit}}}$, where U_{ADCmax} is maximum voltage the ADC is able to measure and N_{bit} is number of the ADC bits. The ADC has an effective resolution equal to 19 bits after application of oversampling. The input voltage range is from $-10V$ to $+10V$, so the resolution is $R_{AD977} = 38.1\mu V/bit$ The minimum ground acceleration to be measured a_{min} is usually selected according to the ambient (cultured)

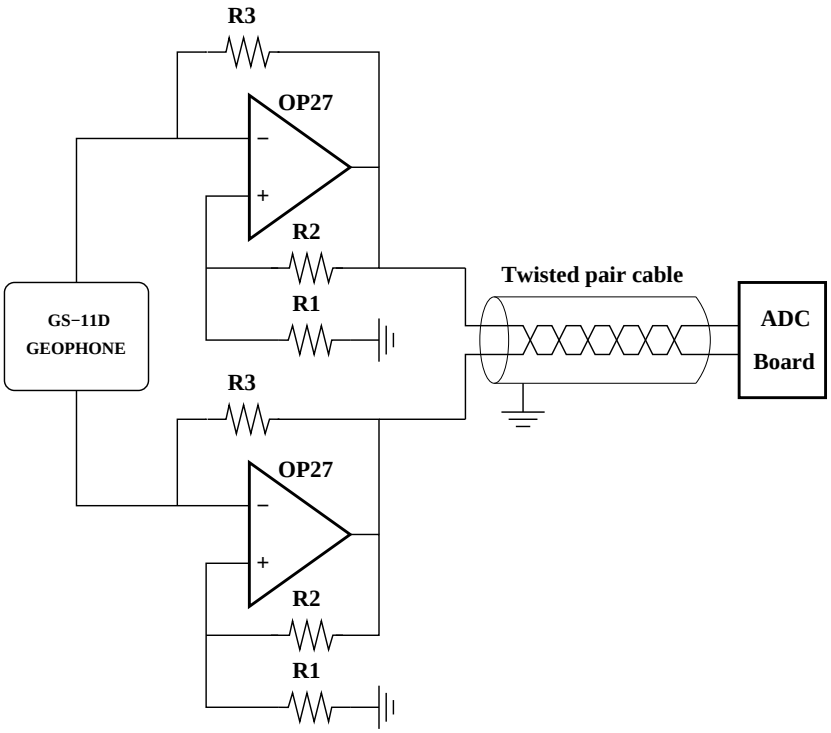

Figure 2.6: Preamplifier design of the SEIS-SCHOOL seismograph . **OP27** - low-noise operational amplifiers, **R1,R2,R3 -** feedback resistors. Amplified signal is transfered to the ADC board through the twisted pair cable.

Parameter	Symbol	Value	Units
Geophone damping	h	10	
Bandwidth	Δf	90	Hz
Sensitivity within bandwidth	S_s	93	$V/(m/s^2)$
Preamplifier gain	A	-500	
A/D Converter voltage resolution	R_{ADC}	38.1	$\mu V/bit$
A/D Converter maximum input voltage	U_{ADCmax}	± 10	V
A/D Converter effective resolution	N_{bit}	19	bit
Positive feedback network resistors values	R_1/R_2	2000/269280	Ω
Negative feedback network resistors values	R_3	211820	Ω

Table 2.2: SEIS-SCHOOL seismograph characteristics.

noise and instrumental noise level. The instrumental noise level is given in the next chapter.

Chapter 3

Instrumental noise

The bandwidth of a seismograph or the range of frequencies it can record is nominally set by the corner frequencies of its transfer function. In practice the bandwidth is defined as the frequency band where signal-to-noise ratio (SNR) does not drop below acceptable limits usually 3 dB (a factor of 2 in power and 1.414 in amplitude). The SNR is defined as:

$$SNR(\omega) = \frac{P(\omega)}{N(\omega)}$$

where $P(\omega)$ is the acceleration spectral density (s.d.) of the input ground acceleration signal in $(m/s^2)/\sqrt{Hz}$, and $N(\omega)$ is the s.d. of the instrumental noise, referred to the equivalent ground acceleration. In the previous chapter the technique for flattening of the geophone response using over-damping preamplifier has been described. As a result the frequency range between the corner frequencies of the transfer function is expanded significantly. However possibly increased level of the instrumental noise can wipe out the large nominal bandwidth achieved due to excessive over-damping, hence it is important to carry out the study of the instrumental noise for the preamplifier.

An important investigation of SNR's, for electromagnetic and feedback seismometers was made by Rodgers (1992). This study includes noise parameters of electromagnetic and feedback seismometers used with both inverting and non-inverting standard

preamplifiers. Some theoretical calculations and practical method of geophone noise measurement are described by Barzilai et al. (1998). A complex study of sensitivity limits for seismometers was made by Riedesel et al. (1990); one important result of this study is: "The noise performance expected from a given amplifier in a circuit for use with a velocity transducer can be calculated to a fairly high degree of accuracy from the amplifier specifications, the circuit parameters, and the sensor's specifications. The level of accuracy is certainly good enough to be able to predict the performance level of any new amplifiers that may become available." This major result has been corroborated by the studies listed above, so accordingly our preamplifier noise study will be based on amplifier circuit and geophone specifications.

The instrumental noise generated by a seismograph consists of two parts - i) the analog noise caused by its analog elements; and ii) the digital noise caused by digitizing errors and digital filters. The analog part is usually dominant, due to refinements in the digital signal processing techniques used nowadays. The analog noise study will be carried out in this chapter. The noise of analog electronic circuits is either generated internally or superimposed by external sources. Like random air currents can generate varying thermocouple voltages that appear as low frequency noise. In our calculations we only take into account the internal noise of electronic components. The internal noise of an electrical circuit can be modeled using ideal voltage and current noise sources connected externally to the circuit inputs, as described in Gray and Meyer (1993). In this model the circuit itself is considered to be noiseless, while the modeled noise is produced only by the external virtual noise sources.

Since noise sources have amplitudes that vary randomly with time and thus can only be specified by a probability density function. Commonly presumed to be Gaussian $G(\mu, \sigma)$ with zero mean (μ) and standard deviation (σ). The instantaneous values are between zero and $\pm\sigma$ 68% of the time. By definition the noise root-mean-square (RMS) value is the standard deviation σ. With multiple noise sources in a circuit, the noise signals must be combined properly to obtain the overall noise signal. If noise sources are independent then their combinational 'effect' will be equal to the root square of

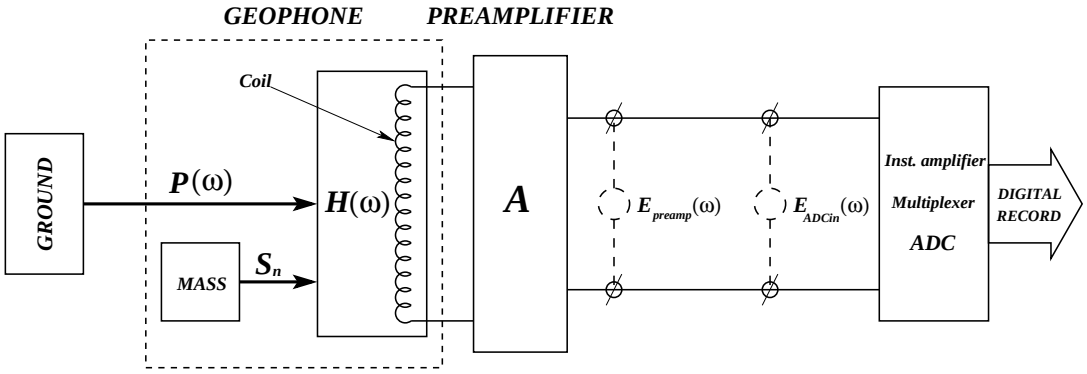

Figure 3.1: Noise sources of the seismograph are shown in the schematic diagram. The ground acceleration is an input signal with the acceleration spectral density (s.d.) $P(\omega)$, the proof mass of the seismometer produces suspension noise acceleration s.d. S_n , the transfer function of the seismometer is $H(\omega)$, the preamplifier generates total noise voltage s.d. $E_{preamp}(\omega)$, the gain of the preamplifier is A, and the A/D converter circuit produces noise voltage s.d. $E_{ADCin}(\omega)$.

their mean square values (Gray and Meyer, 1993). Because the total noise is the RMS value, only the most significant noise sources affect the resulting noise level. This means what weak sources can be ignored in the calculations without significant loss of precision.

The basic noise sources in the seismograph are shown in Figure 3.1. The power s.d. (p.s.d.) of the total instrumental noise produced by the seismograph can be written as:

$$N^2(\omega) = S_n^2 + \frac{E_{preamp}^2(\omega)}{A^2 H^2(\omega)} + \frac{E_{ADCin}^2(\omega)}{A^2 H^2(\omega)} \tag{3.1}$$

where $N(\omega)$ - acceleration s.d of the total instrumental noise referred to the equivalent ground acceleration. The units of all the quantities referred to the equivalent ground acceleration are $(m/s^2)/\sqrt{Hz}$. S_n - acceleration s.d. for the suspension noise of the geophone proof mass, $E_{preamp}(\omega)$ - voltage s.d for the total noise of the preamplifier circuit in $V/\sqrt{Hz}$, $H(\omega)$ - transfer function of the geophone in $V/(m/s^2)$, $E_{ADCin}(\omega)$ - voltage s.d. for the noise of the A/D converter circuit, and A - preamplifier gain. A signal registered by the geophone is mainly affected by the circuit noise before amplification, hence the noise produced by the A/D converter circuit - $E_{ADCin}(\omega)$ can be

dropped without loss of precision.

In order to calculate the total instrumental noise we firstly calculate the suspension noise of the geophone proof mass and then proceed with the noise of the preamplifier circuit. The latter is calculated in two steps; firstly the noise of all passive components (resistors) is calculated and secondly the noise of all active components (operational amplifiers) is obtained. We write the noise voltage p.s.d. of the the preamplifier circuit as:

$$E^2_{preamp}(\omega) = E^2_{Res}(\omega) + E^2_{op}(\omega)$$

where $E_{Res}(\omega)$ - total noise voltage s.d. produced by all resistors, and $E_{op}(\omega)$ - total noise voltage s.d produced by all operational amplifiers. Figure 3.2 depicts the noise sources in the preamplifier circuit.

3.1 Suspension noise of the geophone proof mass

The fundamental limiting factor for the seismometer sensitivity is the noise caused by the Brownian motion of air particles which impact on the suspended mass. The theory here in a seismometer context is presented by Aki and Richards (1980). Who give the acceleration p.s.d. of mass-spring system S_n as:

$$S^2_n = 4kT\frac{\omega_0}{mQ} \tag{3.2}$$

with S_n in $(m/s^2)/\sqrt{Hz}$, Q is the quality factor of the mass-spring system which is equal to $Q = \frac{1}{2h_m}$ where h_m is its mechanical damping factor, k - Boltzmann's constant which is equal to $1.38 \cdot 10^{-23} Joules/K$, T - absolute temperature in degrees Kelvin, ω_0 - resonant angular frequency of the mass-spring system , m - proof mass in kg. For the GS-11D geophone the mechanical damping is $h_m = 0.34$, its resonant angular frequency is $\omega_0 = 2\pi \cdot 4.5Hz$, and the proof mass is $m = 0.024kg$. So at the temperature $T = 293K$ the suspension noise p.s.d. will be:

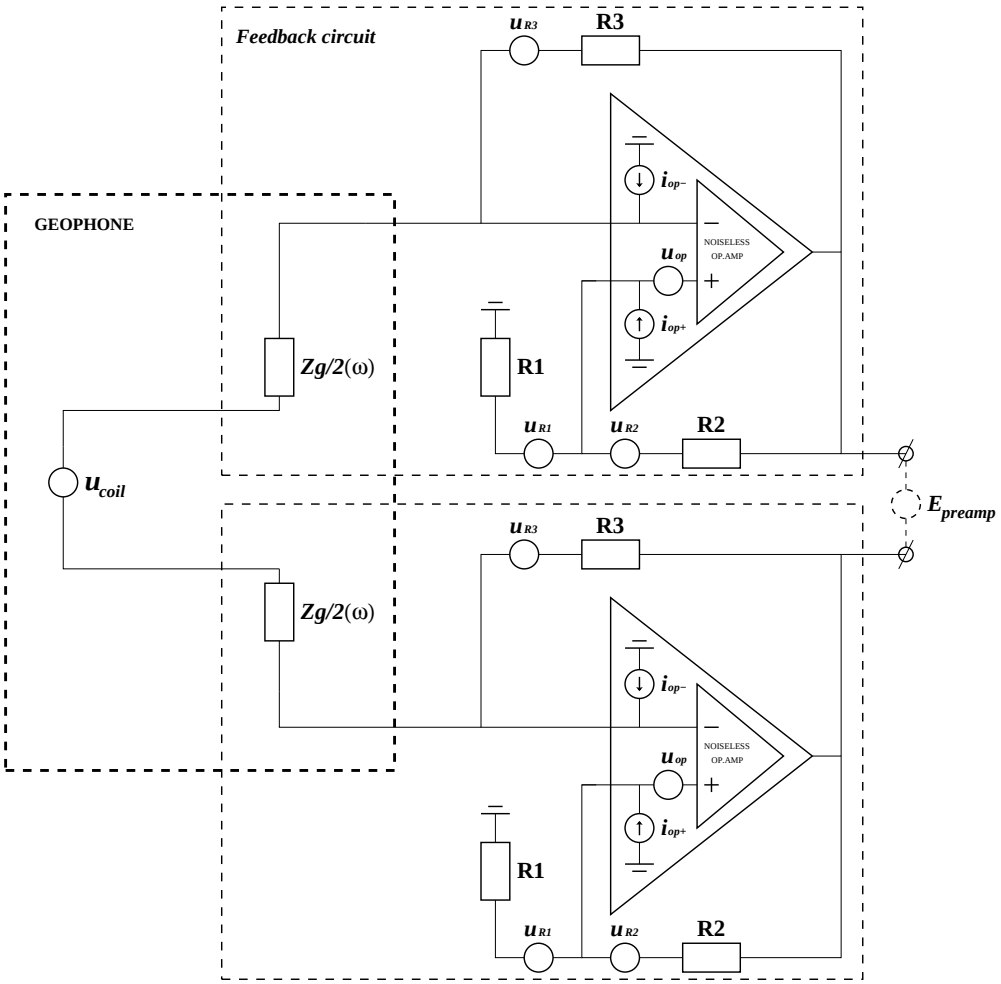

Figure 3.2: Noise sources in the preamplifier circuit depicted in the schematic diagram. u and i represent ideal voltage and current sources, respectively, introduced in the model. u_{op}, $i_{op-}$and i_{op+} represent the noise of operational amplifier circuits, $u_{coil}-$ represents the thermal noise of the geophone coil, u_{R1},u_{R2},u_{R3} represent the thermal noise of relevant resistors, $Z_g(\omega)$ - geophone impedance, E_{preamp} - total noise voltage on the output of the preamplifier.

$$S_n^2 = 4kT\frac{2\pi \cdot 4.5 \cdot 2 \cdot 0.34}{0.024} = 1.3 \cdot 10^{-17}(m/s^2)^2/Hz$$

According to Equation 3.2, in order to decrease the level of the suspension noise one must choose a geophone with higher proof mass and/or lower resonant frequency. The level of the suspension noise is directly proportional to the mechanical damping h_m.

3.2 Johnson's or thermal noise of the electronic dissipative components

Statistical fluctuation of electric charge exists in all conductors, producing random variation of potential between the ends of the conductor. The electric charges in a conductor are found to be in a state of thermal agitation, in thermodynamic equilibrium with the heat motion of the atoms of the conductor. The manifestation of the phenomenon is a fluctuation of potential difference between the terminals of the conductor. (Johnson, 1928)

The thermal noise is due to thermal agitation of the carriers of electricity, hence all dissipative electronic components such as resistor and operational amplifiers produce a noise voltage. This effect was discovered by Johnson (1928) and some theoretical deductions were made by Nyquist (1928). This kind of noise is called Johnson's or thermal noise. The origin of this noise has the same physics as for the mass suspension noise. From Nyquist (1928) the p.s.d. of the noise voltage u is constant and equal to:

$$u^2 = 4kTR$$

where k and T are defined above, R - resistance of the element in $Ohms$. In order to decrease the thermal noise, this equation implies that the values of element resistances should be as low as possible. Dissipative elements in the seismograph are the feedback

resistors R_1,R_2 and R_3 , and the geophone coil resistance R_{coil}. The voltage p.s.d are:

$$u_{R1}^2 = 4kTR_1$$

$$u_{R2}^2 = 4kTR_2$$

$$u_{R3}^2 = 4kTR_3$$

$$u_{Rc}^2 = 4kTR_{coil}$$

respectively. These ideal noise sources affect the preamplifier output differently. The analytic equations for the voltage s.d. on the preamplifier output caused by each independent noise source are calculated in Appendix C for the given preamplifier design. The results are:

$$E_{R1}(\omega) = u_{R1}\frac{2R_2R_3 + R_2Z_g(\omega)}{R_2Z_g(\omega) - 2R_1R_3} \tag{3.3}$$

$$E_{R2}(\omega) = u_{R2}\frac{R_1Z_g(\omega) + 2R_1R_3}{2R_1R_3 - Z_g(\omega)R_2} \tag{3.4}$$

$$E_{R3}(\omega) = u_{R3}\frac{Z_g(\omega)(R_1 + R_2)}{R_2Z_g(\omega) - 2R_3R_1} \tag{3.5}$$

$$E_{Rc}(\omega) = u_{Rc}\frac{2R_3(R_1 + R_2)}{2R_1R_3 - R_2Z_g(\omega)} \tag{3.6}$$

where $E_{R1}(\omega)$, $E_{R2}(\omega)$, $E_{R3}(\omega)$, $E_{Rc}(\omega)$ - voltage s.d. on the preamplifier output caused by the noise of the dissipative elements R_1, R_2, R_3 and R_{coil} respectively, $Z_g(\omega)$ - geophone impedance which is calculated in Appendix A and equal to:

$$Z_g(\omega) = R_{coil} + \frac{-G^2}{\frac{K}{i\omega} - D + mi\omega}$$

where G, K , D, m - geophone physical characteristics described in the Table 2.1. Then the net noise of the seismograph resistive elements will be:

$$E_{Res}^2(\omega) = E_{R1}^2(\omega) + E_{R2}^2(\omega) + E_{R3}^2(\omega) + E_{Rc}^2(\omega)$$

3.3 Noise of the active electronic components

The active electronic elements in the preamplifier circuit are operational amplifiers. Their noise is represented using ideal current sources connected to each input and an ideal voltage source connected in serial to one of the inputs. In Figure 3.2 this sources are depicted as i^2_{op-},i^2_{op+},u^2_{op}, respectively.

The noise of an operational amplifier has two important components; so-called flicker noise dominating at low frequencies and with spectral density roll-off proportional to $1/f$ and the thermal noise dominating at high frequencies with a flat spectra (Section 3.2). The flicker noise is found in all electrical devices which have flowing current through them. Metal film resistors used in seismograph design have negligible amount of this noise. The origin of the noise appears to be imperfections in crystalline structure of semiconductors and it is relatively high in operational amplifiers. According to Gray and Meyer (1993) the voltage and current p.s.d's of the flicker noise in a semiconductor are:

$$E^2_f(\omega) = 2\pi K^2_u/\omega$$

$$I^2_f(\omega) = 2\pi K^2_i/\omega$$

where $E^2_f(\omega)$ and $I^2_f(\omega)$ are, respectively, in units V^2/Hz and A^2/Hz. K_u and K_i are device dependent parameters, ω - angular frequency. An operational amplifier equivalent voltage and current noise sources can be modeled as:

$$u^2_{op}(\omega) = u^2_{op0}\left(1 + \frac{\omega_u}{\omega}\right) \tag{3.7}$$

$$i^2_{op-}(\omega) = i^2_{op+}(\omega) = i^2_{op0}\left(1 + \frac{\omega_i}{\omega}\right) \tag{3.8}$$

where u_{op0} and i_{op0} - are asymptotic high frequency voltage and current noise levels, ω_u and ω_i - are voltage and current corner frequencies. The corner frequency is where the s.d.'s of the flicker and the thermal noise are equal. The above parameters

are usually provided by the manufacturer. For the OP27 operational amplifier these parameters are given in Table 4.1.

From Appendix C the levels of the voltage noise on the preamplifier output as modeled above by the operational amplifier equivalent noise sources are:

$$E_{OPu}(\omega) = u_{op}(\omega)\frac{(R_1 + R_2)(2R_3 + Z_g(\omega))}{2R_3R_1 - R_2Z_g(\omega)} \tag{3.9}$$

$$E_{OPi-}(\omega) = i_{op-}(\omega)\frac{R_3(R_1 + R_2)}{R_2Z_g(\omega) - 2R_1R_3}Z_g(\omega) \tag{3.10}$$

$$E_{OPi+}(\omega) = -i_{op+}(\omega)\frac{2R_2R_3 + R_2Z_g(\omega)}{R_2Z_g(\omega) - 2R_1R_3}R_1 \tag{3.11}$$

where E_{OPu}, E_{OP-}, E_{OP+}, are voltage noise s.d.'s produced on the preamplifier output by equivalent voltage noise source $u_{op}(\omega)$ and current noise sources $i_{op-}(\omega)$, $i_{op+}(\omega)$, respectively. $Z_g(\omega)$ - geophone impedance calculated in Appendix A. So the total voltage noise p.s.d. generated by the operational amplifiers will be:

$$E^2_{op}(\omega) = E^2_{OPu}(\omega) + E^2_{OPi-}(\omega) + E^2_{OPi+}(\omega)$$

3.4 Results

In order to obtain the total noise of the seismograph we sum all independent noise sources referring to equivalent ground acceleration units, that is:

$$N^2(\omega) = S^2_n(\omega) + 2\frac{E^2_{Res}(\omega) + E^2_{op}(\omega)}{A^2 \cdot H^2(\omega)}$$

Where $E_{Res}(\omega)$ and $E_{op}(\omega)$ are the voltage s.d. of the resistive and the active elements, respectively, S_n is the s.d. of the suspension noise of the geophone proof mass. These three term values were calculated in Sections 3.2, 3.3 and 3.2, respectively. A is the preamplifier gain, $H(\omega)$ is the geophone transfer function for ground acceleration. The factor 2 appears because the preamplifier schema is symmetrical what allows us to

calculate the noise for only one operational amplifier presuming that the another one contributes equally.

The numerical results were calculated according to the theory presented in Appendix C. The curves for each independent noise source in the seismograph, as well as its total noise, are shown in Figure 3.3. Due to RMS summation taken for the noise sources only the dominating ones significantly contribute to the net result. For the frequencies below $2Hz$ both the flicker noise and the voltage noise dominate, the increase is proportional to $1/f$. In the frequency band $2-9Hz$ the noise generated by the current flowing through the negative input of the operational amplifier dominates. The relatively high level of this noise is caused by the high resistance of the geophone coil $4000Ohm$. The reason is what the current flows directly through the coil and in this manner generates noise voltage proportional to the coil resistance. For the frequencies above the $9Hz$ the thermal noise of the resistive components becomes dominant due to decrease in the geophone sensitivity. All other noise sources are negligible compare to those mentioned above.

The relatively high current noise is typical for operational amplifiers with bipolar input like the OP27, while this kind is rated as one of the best low noise devices commercially available. There are two possibilities to decrease this noise. Firstly is to decrease the coil resistance by using other geophone types. Secondly is to try to build a preamplifier based on operational amplifiers with FET input, which have extremely low current noise.

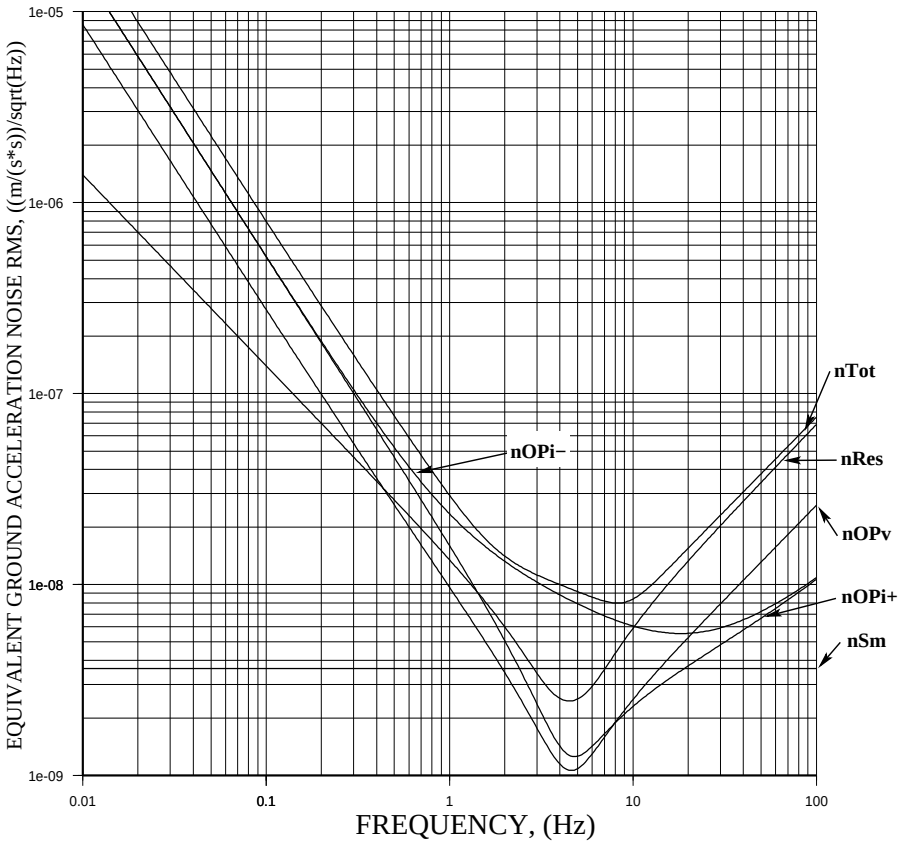

Figure 3.3: Noise generated by electronic components in the SEIS-SCHOOL seismograph, in units of equivalent ground acceleration RMS $(m/s^2)/\sqrt{Hz}$ versus frequency Hz. **nTot -** total noise of the seismograph, **nRes -** total thermal noise of the feedback resistors and the geophone coil , **nOPv -** voltage noise of the operational amplifiers, **nSm -** suspension noise of the geophone proof mass, **nOPi-, nOP+** - current noise of the inverting and non-inverting inputs of the operational amplifiers, respectively.

Chapter 4

Preamplifier design improvement

In the basis of the noise performance analysis carried out in the previous chapter we suggest some improvements for the preamplifier design. The preamplifier modifications suggested in this chapter will provide a lower level of the instrumental noise and forward simplification of the assembling process of the preamplifier. Initially an alternative design with a two-cascade schema is suggested. The first cascade amplifies the geophone signal, and the second cascade transmits the amplified signal through the differential connection line to the A/D converter. In addition the analysis of two different kinds of operational amplifiers JFET and Bipolar is presented.

4.1 Two versus single cascade preamplifier design

The original preamplifier design has a single-cascade schema. The signal from the geophone coil is applied to the differential input and after the amplification transmitted to the differential output of the single cascade. The disadvantage of this design is its high sensitivity to variations of the values of the feedback resistors (Fedorenko pers. com.). A small mismatch in the resistor values causes asymmetries in its output signal

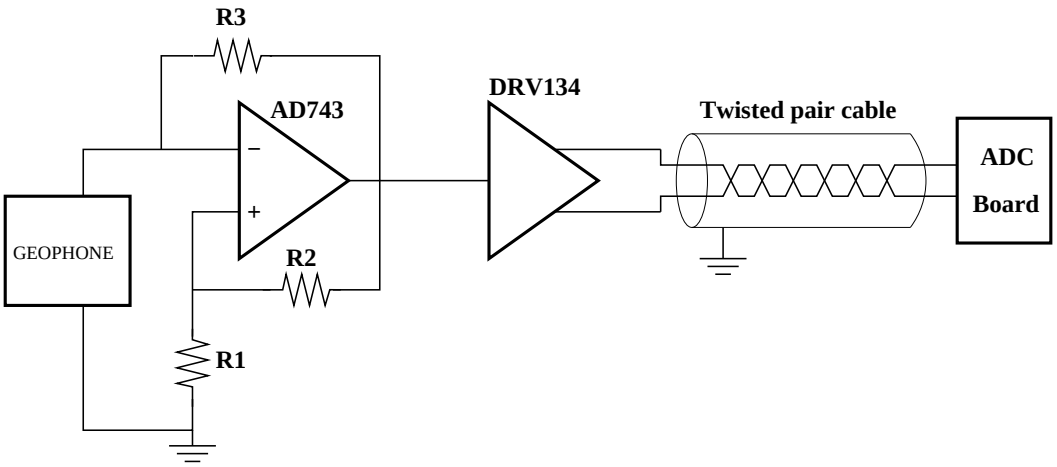

Figure 4.1: Design schematic of the two-cascade JFET input preamplifier. The first cascade is the **AD743** a ultra-low-noise JFET input operational amplifier, the second cascade is the **DRV134** a balanced line driver.

and also changes the amplifier performances in terms of the gain and the input resistance. In other words, the resistors should be selected very carefully. This complicates the assembling process of the preamplifier, and even more so if a feedback thermo-compensation is introduced. Also, note that the differential signal output is vital for a proper transmission through long connection lines to an A/D converter.

The approach here is to build a two-cascade preamplifier. Figure 4.1 shows the schematic of a new design. In the proposed design the geophone coil is connected to the inverting input of the operational amplifier with the another end connected to the ground wire thus creating a definite reference for the signal. In contrast with the old design there each end of the coil was connected to the input of its own amplifier, thus no strong reference point existed. The absence of a strong reference point for the input signal could lower the dynamic range of the preamplifier, due to a possible input un-balance. Note, the only one operational amplifier circuit is required by the new design. The second cascade of the new preamplifier is a 'balanced line' driver which converts the signal from the first cascade to a balanced output pair. This factory made unit for the signal transmission is more robust then any ad-hoc solution. The unit has laser-trimmed resistors for accurate gain and optimum output common-mode

rejection. It easily drives the large capacitive loads associated with long connection lines. Its relatively high output noise level of $400nV/\sqrt{Hz}$ at the 1Hz does not affect the total seismograph noise level, because the signal registered by the geophone is already amplified in the first low-noise cascade. The theory of operation and the noise performance of the proposed preamplifier is described in further details in Appendices B and C.

There are two main differences which influence the new preamplifier noise performance: i) the only one operational amplifier required, so the total noise RMS is decreased by a factor of $\sqrt{2}$, and ii) the whole coil resistance is applied to the negative input of the operational amplifier (instead of one half before), hence the noise sources in the preamplifier will contribute differently to the total noise output. Like according to equation 3.10 a higher coil resistance will cause a higher contribution of the current noise.

4.2 Operational amplifiers performance: JFET versus BIPOLAR

As was stated in the previous section, the total noise level might be higher in the new design due to great influence of the current noise of the **OP27** operational amplifier. This kind of noise is caused by the bipolar input of the **OP27** operational amplifiers. However, there are operational amplifiers based on JFET input are available. Their current noise is almost eliminated at the expense of a higher voltage noise. Because it can significantly affect the total instrumental noise level we analyze the application of JFET input operational amplifiers for the new design.

There are many different operational amplifiers available on the market. For this analysis two representatives of the respective classes JFET and BIPOLAR were selected. Both of which have top noise performances in their respective classes. The **AD743** is the first monolithic JFET operational amplifier to offer the low input voltage noise of an industry-standard bipolar operational amplifier without its inherent input

Parameter	Symbol	**AD743B**	**OP27A**	Units
Input offset voltage	V_{IO}	250	60	μV
Average temperature coefficient for V_{IO}	α_{VIO}	1	0.6	$\mu V/^{\circ}C$
Input offset current	I_{IO}	3.2	50	nA
Input bias current	I_{IB}	16	60	nA
Open loop gain ($R_{LOAD} > 2k\Omega$)	A_{VD}	2000	600	V/mV
Input voltage noise ($f = 10kHz$)	u_{op0}	3	2.9	$nV/\sqrt{Hz}$
Input current noise ($f = 1kHz$)	i_{op0}	6.9	400	$fA/\sqrt{Hz}$
Input voltage noise corner frequency	f_u	26.5	2.7	Hz
Input current noise corner frequency	f_i	100	140	Hz
Power supply quiescent current	I_{CC}	10	3.5	mA

Table 4.1: AD743B and OP27A operational amplifiers worst case parameters over the industrial temperature range of $-40^{\circ}C$ to $+85^{\circ}C$.

current errors. The **OP27** is an industry-standard very low noise high speed bipolar operational amplifier, which is used in the original design of the preamplifier. Operational specifications for both of them are given in Table 4.1.

While JFET input operational amplifiers have superior current noise parameters there are some disadvantages exist. One is the input offset voltage V_{IO} which is 5 times higher when in the bipolar. That is attributed to the transconductance of the JFET, which is lower than of the bipolar transistors (Gray and Meyer, 1993). This will cause $V_{OF} = 0.12606V$ as a worst case offset output voltage and temperature drift of $0.51mV/^{\circ}C$ for a two-cascade amplifier with gain $A = -500$, or doubled for a one-cascade version. The offset can be eliminated using null adjustment pins; this procedure is standard and well described in Nguyen and Smith (2000). Another disadvantage is that the voltage noise has a higher corner frequency so it will be higher at the low frequencies, see equations (3.7) and (3.8) for the noise spectral density of operational amplifiers. The advantages of the JFET input are: i) the open loop gain is higher thus providing less signal distortion in the preamplifier itself, and ii) the current noise is almost eliminated.

4.3 Optimal preamplifier design for the GS-11D $4k\Omega$ geophone

From above, we have that four different preamplifier designs can be suggested namely:

1. one-cascade bipolar input preamplifier
2. one-cascade JFET input preamplifier
3. two-cascade bipolar input preamplifier
4. two-cascade JFET input preamplifier

We analyze which one is the best in terms of noise performances when it is applied to the GS-11D $4k\Omega$ geophone. Firstly, we calculate a total instrumental noise curve for each of them, using the techniques described in the previous chapter. The results are shown in Figure 4.2 which cleanly demonstrates that the fourth design solution - the two-cascade JFET input preamplifier has the best noise performance.

4.4 Influence of the geophone coil resistance

Next step was to analyze the noise performance of the suggested preamplifiers for different geophone coil resistances, since this factor affects the instrumental noise (Appendix C). In order to display this dependence, we calculate noise level curves for coil resistances changing from 100Ω to $10k\Omega$. Here the geophone generator constant G is taken proportional to the square root of the coil resistance $G = K_g\sqrt{R_{coil}}$ (Riedesel et al., 1990), with K_g - normalized geophone transduction constant. This implies that the geophone mechanical construction and the magnet parameters are the same, hence only the number of radial layers of the coil is changed in order to vary the coil resistance. This is usually the case when a geophone manufacturer provides a geophone model with different coil resistances. The results of these calculations, are shown in Figure 4.3. The SNR is calculated for the input ground acceleration power spectral

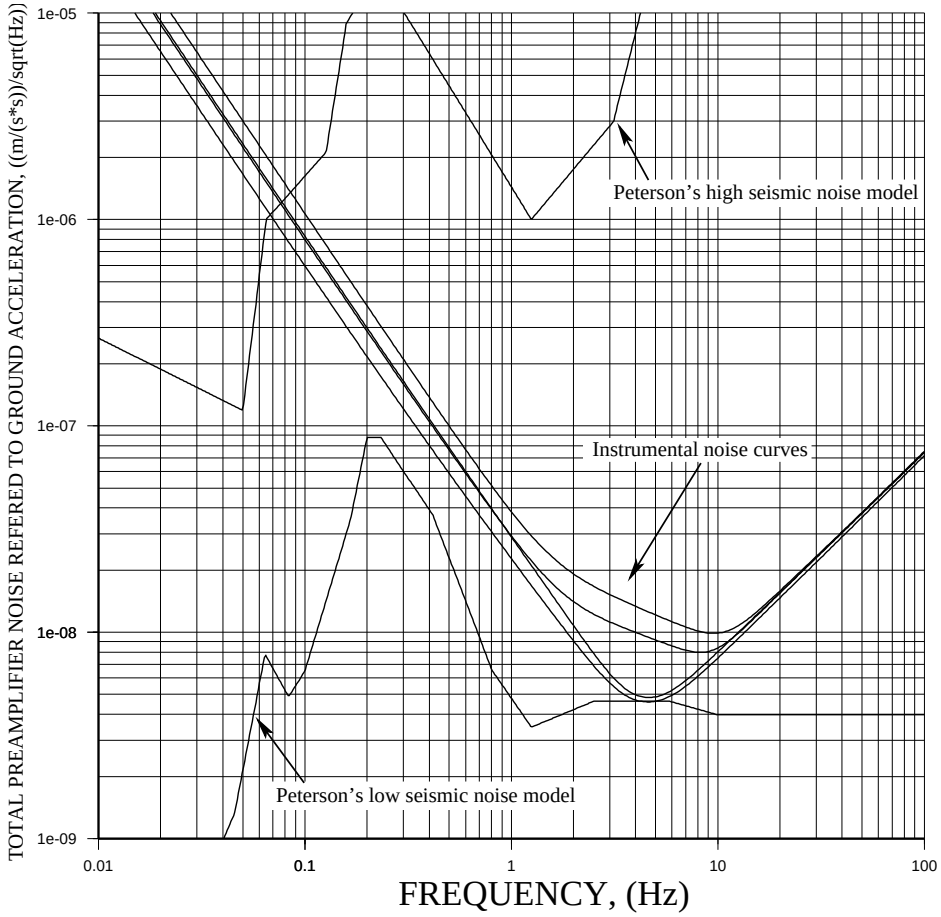

Figure 4.2: Curves show total noise of preamplifiers for different design solutions referred to equivalent ground acceleration $(m/s^2)\sqrt{Hz}$. From top to bottom the curves display the noise of: i) two-cascade bipolar, ii) one-cascade bipolar, iii) one-cascade JFET, and iv) two-cascade JFET preamplifiers. The levels of high and low Peterson's seismic noise models are also shown for the reference.

density $P^2(\omega) = 1.6 \cdot 10^{-17}(m/s^2)^2/Hz$, which is approximately equal to Peterson's low seismic noise model above frequency $1Hz$. The diagrams display that JFET preamplifiers give higher SNR values for higher coil resistances, and the two-cascade schema is better. While for bipolar preamplifiers the coil resistance about 500Ω are optimal and the one-cascade schema is better.

Figure 4.4 shows the spectral density of the instrumental noise at $1Hz$ versus coil resistance, for all four preamplifier designs. For coil resistances below $3k\Omega$ bipolar input preamplifiers give a better noise performance. For higher coil resistances JFET input preamplifiers are preferred. For JFET preamplifiers the two-cascade schema is always less noisy. While for bipolar input preamplifiers when applied to coil with resistances less then $1k\Omega$ the two-cascade schema is preferred, but for higher resistances the one-cascade schema gives a better result.

To summarize the noise analysis for the GS-11D Geospace geophone, which is available in two versions with 380Ω and $4k\Omega$ coil resistances, the best noise performance will be achieved when using a two-cascade JFET input preamplifier with $4k\Omega$ coil resistance. The spectra for noise level of this preamplifier is shown on Figure 4.2. From the figure for frequencies below $1Hz$ the voltage noise of the operational amplifier dominates, while for higher frequencies the total thermal noise of the resistive elements is the most important.

4.5 Conclusions

An alternative preamplifier design based on a two-cascade schema was proposed and four different design solutions for the GS-11D geophone have been analyzed. The comparative analysis of the one- and two-cascade schemas shows what for JFET preamplifiers the two-cascade schema gives a better noise performance, while for bipolar preamplifiers it is the one-cascade schema. The analysis of the influence of a geophone coil resistance on the noise performances of a preamplifier showed what bipolar input preamplifiers give a better performance for low coil resistances, while JFET in-

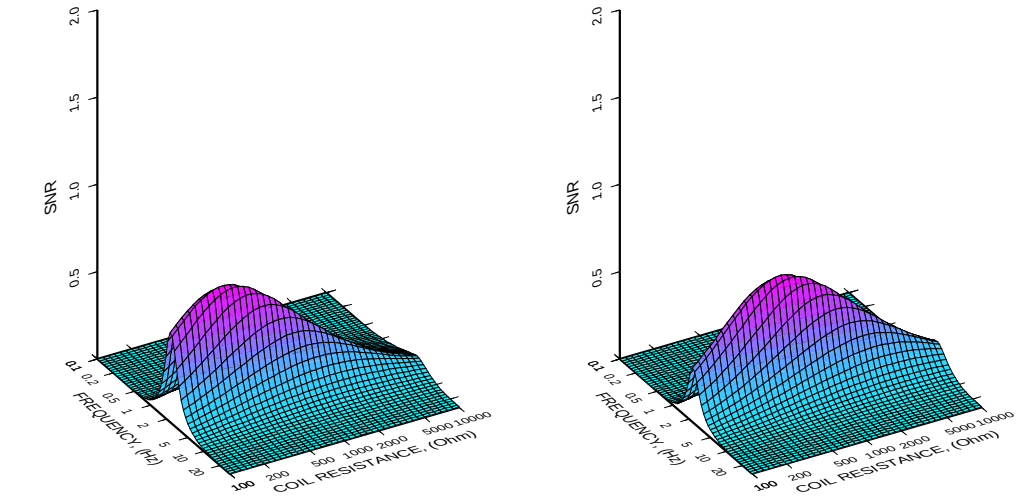

a) b)

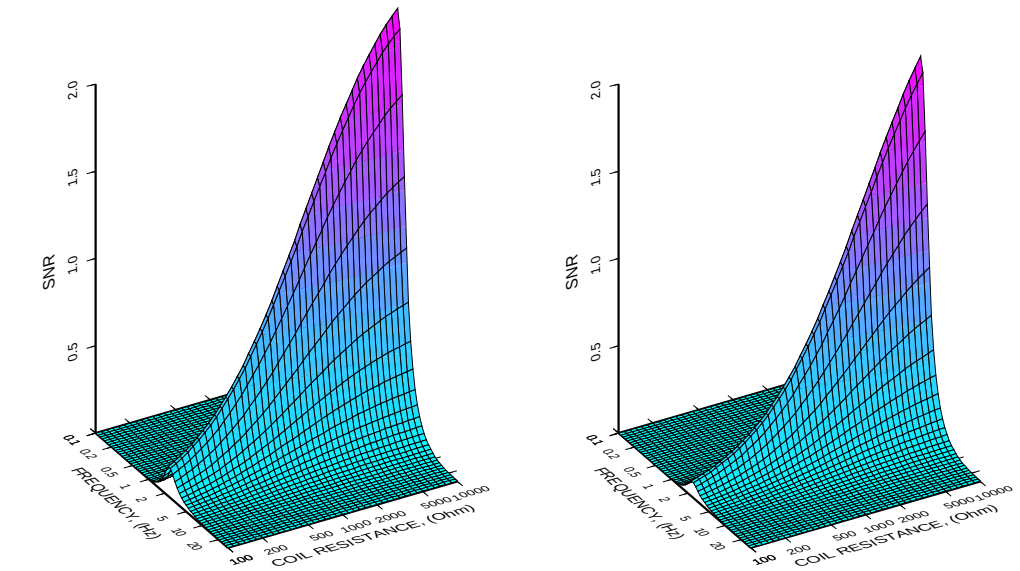

c) d)

Figure 4.3: SNR versus frequency and coil resistance. a) bipolar input two-cascade preamplifier, b) bipolar input one-cascade preamplifier, c) FET input two-cascade preamplifier, d) FET input one-cascade preamplifier.

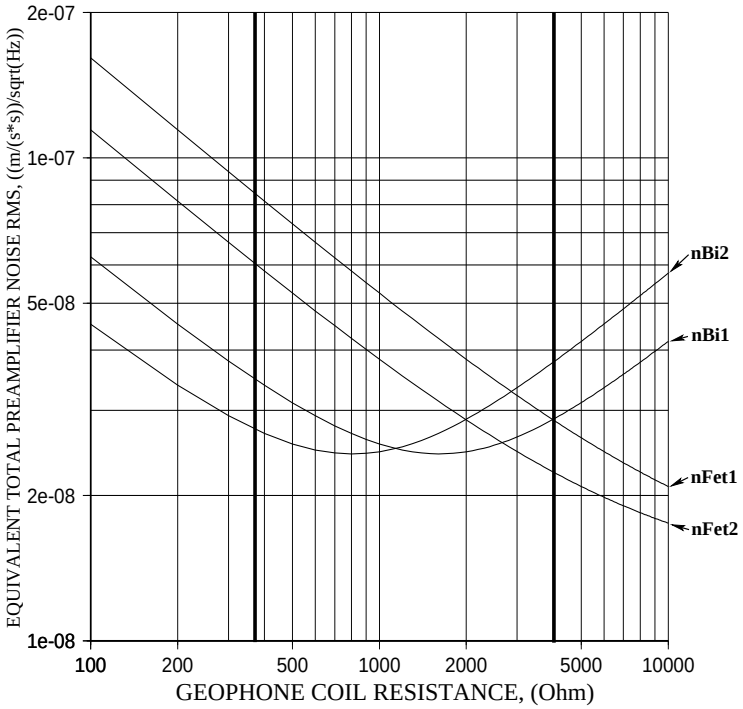

Figure 4.4: Spectral density of the total noise of preamplifiers $(m/s^2)/\sqrt{Hz}$ at $1Hz$ for different design solutions versus geophone coil resistance. The geophone generator constant G is taken proportional to the coil resistance. **nBi2 -** two-cascade bipolar input preamplifier, **nBi1 -** one-cascade bipolar input preamplifier, **nFet1 -** one-cascade JFET input preamplifier, **nFet2 -** two-cascade JFET input preamplifier. "Thick" lines represents Geospace GS-11D geophone models with coil resistances equal to 380Ω and $4k\Omega$, respectively.

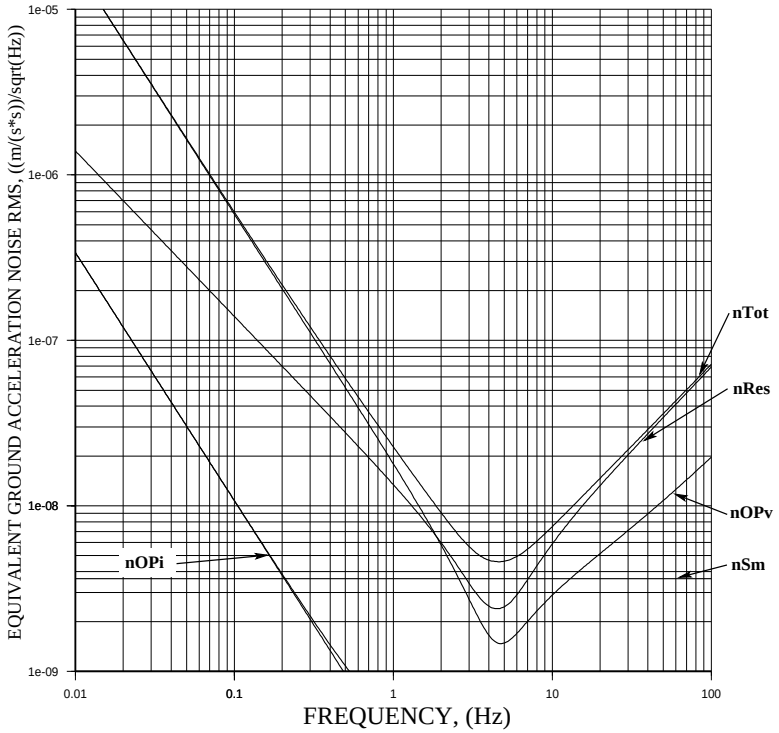

Figure 4.5: Spectral density of the instrumental noise of the two-cascade JFET input preamplifier referred to equivalent ground acceleration RMS $(m/s^2)/\sqrt{Hz}$ versus frequency Hz. **nTot -** total seismograph analog noise, **nRes -** total thermal noise of feedback resistors and geophone coil , **nOPv -** voltage noise of operational amplifiers inputs, **nSm -** geophone mass suspension noise ,**nOPi** current noise of the inverting and non-inverting inputs of the operational amplifier

put preamplifiers are better for high coil resistances. The JFET preamplifier with the two-cascade shema shows the best instrumental noise performance when applied to the $4k\Omega$ version of the GS-11D geophone.

Chapter 5

Inverse-filter technique for flattening of the geophone response

In previous chapters the over-damping technique for flattening of the geophone response was described. One significant disadvantage of this method is the dependence of the transfer function of the seismograph on the ambient temperature. A way of avoiding this is through feedback thermo-compensation which quite complicated for practical realization, as it requires low tolerance resistors for its implementation. An other approach for flattening the seismometer response is through so-called inverse-filtering technique. The inverse filter here is a preamplifier that selectively provides progressively higher amplification for lower and higher frequencies. In this chapter is demonstrated how to apply this method to the GS-11D geophone in order to enhance its frequency bandwidth.

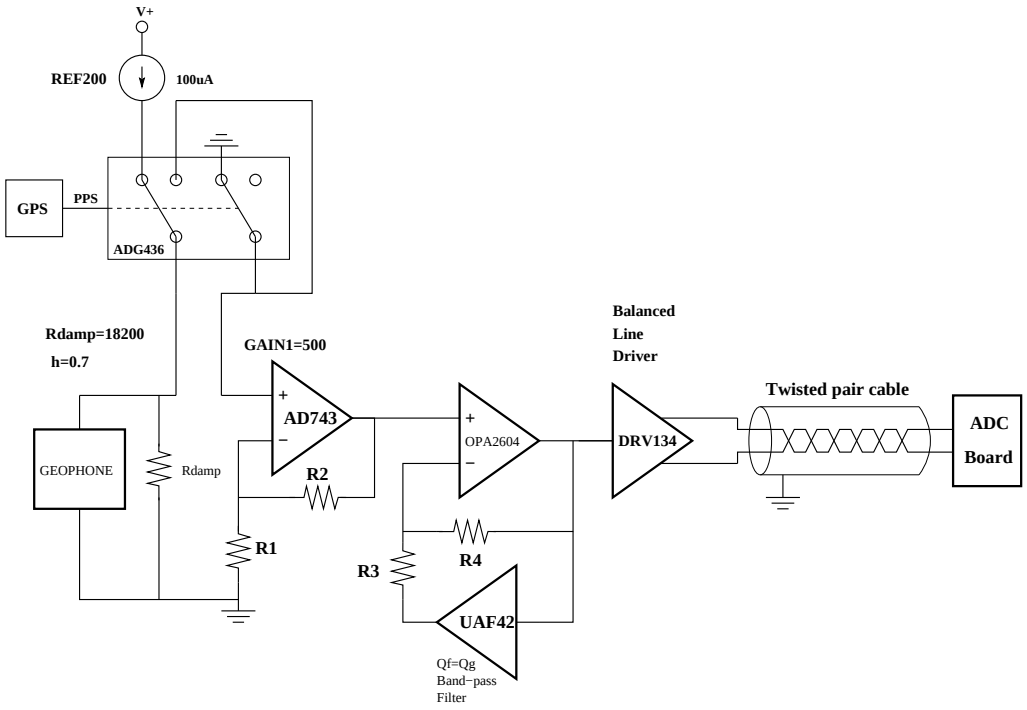

Figure 5.1: Schematic view of the inverse filer preamplifier together with calibration module schematic. Here **AD743 -** ultra-low-noise JFET input operational amplifier, **OPA2604 -** low-noise low-power operational amplifier, **UAF42 -** universal active filter configured as second order bandpass filter with resonant frequency and Q equivalent to geophone transfer function for acceleration, **DRV134 -** balanced line driver, **REF200 -** high precision $100\mu A$ current source, **ADG436 -** dual SPDT switch.

5.1 Inverse-filtering preamplifier design

The inverse-filtering preamplifier transfer function is actually an inverted transfer function of the geophone. The schematic diagram of the preamplifier is illustrated in Figure 5.1. The geophone damping factor $h = 0.7$ is achieved using a damping resistor $R_D = 18200\Omega$. Higher damping will cause dependence of the geophone transfer function on temperature fluctuations, as was shown in Section 2.2. The signal from the geophone coil passes to the 'first stage' very-low-noise amplifier, which has a flat transfer function. The gain is set as high as possible, but its upper limit is adjusted is such a way to avoid the A/D converter clipping at the resonant frequency. The signal after amplification is very little affected by the noise in the following cascades. After the amplification the signal passes to a correcting amplifier, which amplifies signal frequencies around the resonant and has unity gain at the resonant frequency. The correcting amplifier is build from an operational amplifier with a band-pass filter of second order in its negative feedback network. This because a geophone acts as a second order band-pass filter when it is used to measure ground acceleration. The transfer function of the band-pass filter is inverted. The quality factor of the band-pass filter is equal to geophone quality factor $Q_f = Q_g = \frac{1}{2h}$, where h is the geophone damping as before. As a band-pass filter a Salen-Key topology second order band-pass filter can be used, or in order to simplify the preamplifier assembling process, the Texas Instruments UAF42 universal active filter. The last one has the software for calculation of standard 1% tolerance resistor values from desired resonant frequency and given the Q factor. The bandwidth of the inverse filter is limited by the resistors R_2 and R_3. After spectral correction the signal goes to a differential line driver, which transmits the signal through the connection cable to the A/D converter board.

5.2 Numerical simulation results

The numerical modeling of the given preamplifier in combination with different geophones has been performed using SPICE simulation environment. The obtained results

show that for a proper design it is necessary to know precisely values of the geophone damping and the resonance frequency. The GS-11D resonance frequency is $4.5Hz$ with a factory tolerance of $\pm 0.75Hz$ causing a variation of 20% in the preamplifier gain in a given frequency band. So it is impossible to achieve precisely the required gain using only geophone specification values.

5.3 Current step-release calibration technique

However, pre-calibration techniques could be applied to obtain seismometer parameters. They allow precise measurement of the resonance frequency and the mechanical damping for a seismometer. While geophones usually do not have a calibration coil, a calibration method called 'current step-release' can be applied. It measures the transient response of the signal coil when a step of current is released (Asten, 1977); Houliston et al., 1982; MacArthur, 1985; Menke et al., 1991; Rodgers et al., 1995; Fedorenko et al., 1999. The resulting transient has a simple analytic dependence on the damped generator constant, resonant frequency, and damping factor of the geophone. This method does not require a calibration coil. Only the seismometer mass (from the manufacturer) and the applied current (measured) need to be known for the complete calibration. In the given design this method can be easily applied because the preamplifier has almost infinite input resistance. The calibration unit is shown in Figure5.1 as a ADG436 circuit connected to a GPS receiver.

5.4 Conclusions

An overview of an alternative technique for flattening of the geophone response is presented by an example of the practical realization. The numerical modeling of the proposed design showed the strong dependence of the preamplifier transfer function on the value of geophone resonance frequency. The factory specified tolerance of the geophone parameters is to high for application of this technique. The current step-release cali-

bration technique can be used in order to obtain precise geophone parameters required by the proposed technique.

Chapter 6

Conclusion and discussion

The instrumental noise calculation was based on the theoretical model of the overdamping preamplifier applied to a geophone. The results show that the noise performance of geophone-based seismographs are comparable with those of short period seismometers. Referring to Peterson's high seismic noise model, the geophone-based seismograph is able to record seismic signals with frequency down to $0.1Hz$ or with highest period of 10 seconds. The modeling shows that for frequencies below $10Hz$ the major noise source is the current noise of the operational amplifiers, while for higher frequencies the thermal noise of the resistive components dominates. So an alternative type of operational amplifier may improve the noise performance for low frequencies. A new preamplifier design based on JFET type operational amplifiers is proposed in this work. It provides lower noise levels for frequencies less then $10Hz$, and simplifies the practical realizations of a preamplifier.

The theoretical results may be insignificantly biased by the simplifications of the model used in the calculations. The model drops such effects as external electromagnetic sources, thermocouple voltages caused by ambient temperature fluctuations, insignificant sources of noise in electronic circuits, none zero resistances of connection wires, and finite open loop amplification of the operational amplifiers. For a further investigation of the noise performance an experimental measurement is required. It can

be done using the technique described in Barzilai and VanZandt (1998). The technique is based on the analysis of the records done by two similar instruments which share the same location. The instrumental noise level is obtained through correlation analysis of the records.

For comparative analysis an overview of another technique for modification of the geophone response is given. This technique does not suffer from temperature variations as the original one, but it is sensitive to precise values of the geophone resonance frequency and generator constant.

Bibliography

[1] Aki, K., Richards, P., 1980. Quantitative seismic theory and methods. W.H. Freeman, San Francisco.

[2] Barzilai, A., Van Zandt, T., 1998. Technique for measurements of the noise of a sensor in the presence of large background signals. Review of scientific instruments, Vol. 69, Num. 7.

[3] Johnson, J., 1928. Thermal agitation of electricity in conductors. Phys. Rev. Vol. 32, 97-109.

[4] Gray, P., Meyer, R, 1993. Analysis and design of analog integrated circuits. John Willey & Sons, New York.

[5] Horowitz, P., Hill W., 1990. The art of Electronics. Cambridge University Press, Cambridge.

[6] Nguyen B., Smith D., 2000. Nulling input offset voltage of operational amplifiers. Texas Instruments Application Report, SLOA045.

[7] Nyquist H., 1928. Thermal agitation of electric charge in conductors. Physical review, Vol. 32.

[8] Riedesel, M., Moore, R., Orcutt, J., 1990. Limits of sensitivity of inertial seismometers with velocity transducers and electronic amplifiers. Bull. Seismol. Soc. Am., Vol. 80, 1725-1752.

[9] Rodgers, P., 1992. Frequency limits for seismometers as determined from signal-to-noise ratios. Part 1. The electromagnetic seismometer., Bull. Seismol. Soc. Am., Vol. 82, No.2, 1071-1098.

[10] Rodgers, P., 1992. Frequency limits for seismometers as determined from signal-to-noise ratios. Part 2. The feedback seismometer., Bull. Seismol. Soc. Am., Vol. 82, No.2, 1099-1123.

[11] Rodgers, P, 1993. Maximizing the signal-to-noise ratio of the electromagnetic seismometer: the optimum coil resistance, amplifier characteristics, and circuit. Bull. Seismol. Soc. Am., Vol. 83, No. 2, 561-582.

[12] Rodgers, P., 1994. Self-noise spectra for 34 common electromagnetic seismometer/preamplifier pairs. Bull. Seismol. Soc. Am., Vol. 84, No. 1, 222-228.

[13] Rodgers, P., 1995. Signal-coil calibration of electromagnetic seismometers. Bull. Seismol. Soc. Am., Vol. 85, No. 3, 845-850.

Part II

Advanced e-learning modules for high schools: applying modern Web-technologies

Advanced e-learning modules for high schools: applying modern Web-technologies

by

Mikhail E. Boulaenko and Eystein S. Husebye

Abstract: This paper highlights the SEIS-SCHOOL project e-learning modules conceptual design and gives brief description of its practical application. We start with an overview of available Web-technologies for creation of advanced electronic learning modules. Then demonstrate that such technologies and freeware suffice for creation of advanced e-learning modules. Important here is that costly commercial software is not needed for compliance to high-level e-learning standards regarding module's accessibility, durability, interoperability, and content reusability.

Institute of Solid Earth Physics, University of Bergen

Allégaten 41, 5007 Bergen, Norway

December, 2002

Chapter 7

Introduction

Our ability to use technology opens new opportunities for exploring ways to teach and learn more effectively. The concept of using technology in learning is not new; the format of the technology is just changing. Technology aids, ranging from books, slide rules, calculators, televisions to present day personal computers (PC's) have supported class room teaching for years. Changes in technology have been at a non-linear rate and now provide new options to deliver far more effective, personalized lectures than in the past. Today's generation of children are growing up with a different expectation of technology's role in their lives, with the minimum acceptable level of graphical quality and interactivity being driven from video games (Brogan, 1999).

Today, one can buy a Pentium computer system, with high quality sound and video for less than $1,000. This provides a robust platform, which can support full motion video, audio, and powerful software routines. While hardware developments have progressed according to Moore's Law (former IBM research scientist), software has evolved in stages and at a much slower pace. According to Moore's Law, the capacity of a computer chip doubles every 18 months. If software development tools had advanced similarly, we would have had smaller code bases, with tools that allow for much easier and fast developments (Lehman, 1997).

Over the past 20 years, there have been four different generations of instructional

ADL	Advanced Distributed Learning
CAM	Content Aggregation Model
CM	Content Model
DoD	Department of Defense
FO	Formatting Objects
LMS	Learning Management System
SCO	Sharable Content Object
SCORM	Sharable Content Object Reference Model
SVG	Scalable Vector Graphics
W3C	World Wide Web Consortium
WWW	World Wide Web
XML	eXtensible Markup Language
XSL	Extensible Stylesheet Language

Table 7.1: Acronym Listing

software, following the availability of different operating systems. First-generation products were text-based, typically running under DOS. Second-generation products were built with rudimentary graphics and provided practice functionality instead of instruction. Third generation products were designed to deliver a rich-media learning experience commonly via interactive CD-ROMs. These products included engaging multimedia, such as interactive encyclopedias, which in turn offered limited instruction. Fourth generation products are available now. These products utilize audio, graphics, animation and text in a way that has been proven to deliver increases in learning retention by stimulating both right and left brain activities. Animation and graphics, combined with programmed logic, allow software to adapt to user input, providing a more complete learning environment (Brogan, 1999).

In this work we give an overview of modern Web-based technologies available for creation of interactive learning experiences. We present our own approach to creation of e-learning modules based on open standards and compliant to high level e-learning standards. Note, acronyms are extensively used in modern Web-technologies and those used in this article are listed in Table 7.1.

Chapter 8

SCORM standard for Web-based e-learning

The Department of Defense (DoD/USA) launched in 1997 the Advanced Distributed Learning (ADL) initiative to develop a DoD-wide strategy for using learning and information technologies to modernize education and training within the government. Its intention was also to promote cooperation between government, academia and business to develop e-learning standardization. The ADL initiative has defined high-level requirements for learning content, including its reusability, accessibility, durability and interoperability to leverage existing practices, promote the use of technology-based learning and provide a sound economic basis for investment.

The Sharable Content Object Reference Model (SCORM^{TM}) defines a Web-based learning "Content Aggregation Model" and "Run-time Environment" for learning objects. At its simplest, it is a model that references a set of interrelated technical specifications and guidelines designed to meet the DoD's high-level requirements for Web-based learning content. The SCORM requirements:

- **Accessibility:** the ability to locate and access instructional components from one remote location and deliver them to many other locations.

- **Interoperability:** the ability to take instructional components developed in one location with one set of tools or platform and use them in another location with a different set of tools or platform. There are multiple levels of interoperability.
- **Durability:** the ability to withstand technology changes without costly redesign, reconfiguration or recoding.
- **Reusability:** the flexibility to incorporate instructional components in multiple application and contexts.

The SCORM assumes a Web-based infrastructure as a basis for technical implementation. ADL made this assumptions for several reasons:

- Web-based technologies and infrastructure are rapidly expanding and provide a mainstream basis for learning technologies.
- Web-based learning technology standards do not yet exist in widespread form.
- Web-based content can be delivered using nearly any medium (e.g CD-ROM, standalone systems and/or as networked environments).

This approach embraces industry's transition to common content and delivery formats.

8.1 SCORM Content Aggregation Model

The SCORM Content Aggregation Model (CAM) represents a pedagogically neutral means for designers and implementers of instruction to aggregate learning resources for the purpose of delivering a desired learning experience. A learning resource is any representation of information that is used in a learning experience. The CAM is made up of following components:

- **Content Model:** Nomenclature defining the content components of a learning experience.

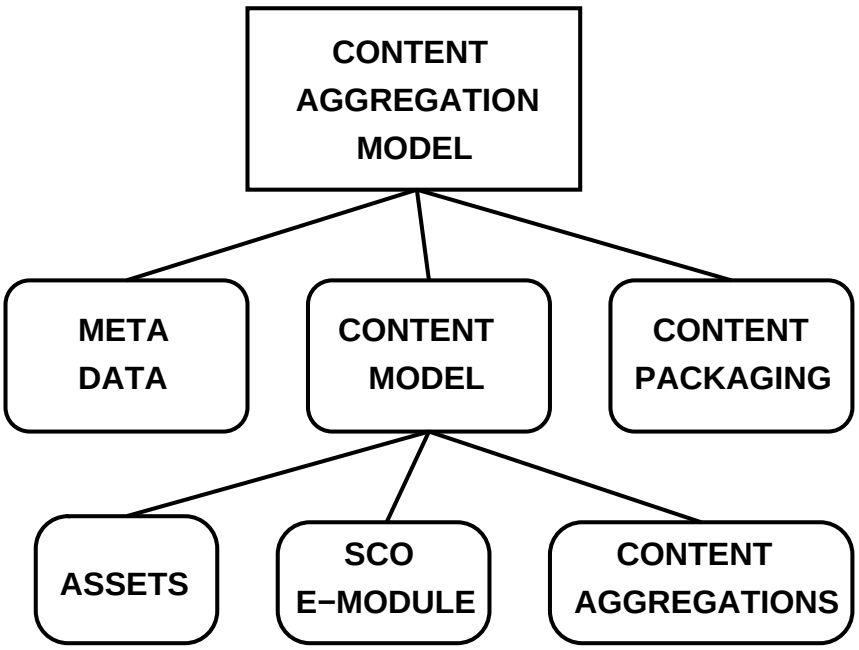

Figure 8.1: SCORM Content aggregation model components.

- **Meta-data:** A mechanism for describing specific instances of the components of the content model.
- **Content Packaging:** Defines how to represent the intended behavior of a learning experience (Content Structure) and how to package learning resources for movement between different environments. (Content Packaging).

8.2 SCORM Content Model

The SCORM Content Model (CM) describes components used to build a learning experience from reusable learning resources. It is made up of the following components:

- **Assets:** the most basic form of learning content, the electronic representation of text, images, animations, video, sound, or other pieces of data.
- **Sharable Content Objects (SCO):** a collection of one or more Assets that in-

clude a specific launchable asset that utilizes the SCORM RTE to communicate with LMS's. A SCO represents lowest level of granularity of learning resources that can be tracked by LMS. To be reusable a SCO should be independent of learning context and subjectively small unit.

- **Content Aggregation:** a map that can be used to aggregate learning resources into a cohesive unit of instruction, apply structure and associate learning taxonomies. The content structure defines taxonomic representation of the learning resources. The Content Aggregation defines the content structure that provides the mechanism for defining the sequence that learning resources are to be presented to the user.

The instances of the CM can be referred to related Meta-data to allow for search within online repositories, thereby enhancing opportunities for reuse.

Chapter 9

XML the Web-based standard for content storage and exchange

Extensible Markup Language, abbreviated XML, describes format for documents containing structured data. Markup encodes a description of the document's storage layout and logical structure. XML provides a mechanism to impose constraints on the storage layout and logical structure. XML was developed by an XML Working Group formed under the auspices of the World Wide Web Consortium (W3C) in 1996. It was chaired by Jon Bosak of Sun Microsystems with the active participation of an XML Special Interest Group also organized by the W3C. The design goals for XML are:

- XML shall be straightforwardly usable over the Internet
- XML shall support a wide variety of applications
- XML documents should be human-legible and reasonably clear
- It shall be easy to write programs which process XML documents

- XML documents shall be easy to create

XML, has become extremely popular and is both widely and reliably implemented. In current developments of Web-based applications the XML is the most widely used standard. The W3C has developed the standard way of processing XML content - Extensible Stylesheet Language (XSL). Given a class of arbitrarily structured XML documents, designers use an XSL stylesheet to express their intentions about how that structured content should be presented; that is, how the source content should be styled, laid out, and paginated onto some presentation medium, such as a window in a Web browser or a hand-held device, or a set of physical pages in a catalog, report, pamphlet, or book.

9.1 SVG the Web-based delivery format

Scalable Vector Graphics (SVG) is a language for describing interactive two-dimensional graphics in XML. To be scalable means to increase or decrease uniformly. In terms of graphics, scalable means not being limited to a single, fixed pixel size. Vector graphics contain geometric objects such as lines and curves. This gives greater flexibility compared to raster-only formats (such as PNG and JPEG) which have to store information for every pixel of the graphic. SVG can also integrate raster images and can combine them with vector information such as clipping paths to produce a complete illustration. Most existing XML document formats represent either textual information, or represent raw data such as financial information. They typically provide only rudimentary graphical capabilities. SVG fills a gap in the market by providing a rich, structured description of vector and mixed vector/raster graphics. SVG drawings can be interactive and dynamic. Sophisticated applications of SVG are possible by use of a supplemental scripting language. SVG leverages and integrates with other W3C specifications and standards efforts. By being written in XML, SVG builds on this strong foundation and gains many advantages such as a sound basis for internationalization, powerful structuring capability, an object model, and so on.

Chapter 10

SEIS-SCHOOL e-module conceptual model

In the context of this paper an e-learning module will be a SCORM Sharable Content Object and thereby inherits all its properties and restrictions. For a SCO the SCORM defines only it external properties and interface with LMS. The internal knowledge structure is up to e-module producer to define. This approach allows existence of various kinds of e-learning modules. They may be classified as simple and advanced learning objects (Hesthammer et al., 2001b). The simple learning objects are created using standard office software like Microsoft Word or PowerPoint. The advanced learning objects require complicated and expensive authoring tools like Macromedia Authorware.

Our approach to e-modules design is based on modern Web-technology and open standards. We have created XML grammar which fully describes an E-module content. The e-module content model is made up of the following components:

- **Assets:** fully compliant to SCORM standard. Currently supported: raster images, vector SVG figures and animations, control buttons, internal and external hyperlinks, text-boxes, quizzes.

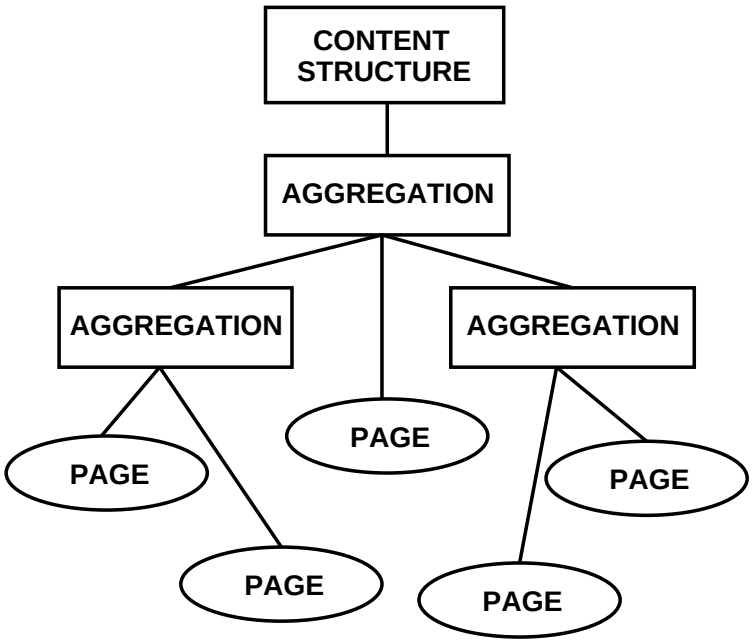

Figure 10.1: SEIS-SCHOOL e-module structure.

- **Pages:** aggregations of assets, lowest granularity units accessible from the module menu
- **Aggregations:** structural elements, may contain one or more Pages
- **Module structure:** tree-like structure of the module made up of Aggregations and Pages, defines the module navigation menu.
- **Learning paths:** define the sequence of Pages presented during learning process. There may be many learning paths for one module.

The XML document with e-module content is processed using XSL stylesheet to create desired SVG output. Thus content producers don't need to be aware of module design. The SVG output is created in the form of a stand-alone web-page which can be viewed via a web-browser. The graphical design and navigation for the module can be easily altered without disturbing its content. The text-boxes are created using XSL Formatting Objects (XSL-FO) Processor by the Apache Software Foundation. This XSL-FO Proces-

sor is the world's first formatter driven by XSL formatting objects and the world's first output independent formatter.

Comparing "simple learning objects" with our design one can notice similar differences as between popular text processors Microsoft Word and LaTeX. The creator of MS Word document must be aware of how the text will be printed on paper, while he has full control of the presentation the possibilities for content reuse are poor or absent. In the case of LaTeX or LyX the writer must only define structure of the document in form of chapters, paragraphs, etc. The final presentation is created applying the desired stylesheet, thereby multiple presentations of the same content (printed forms, web-page, simple text file, etc.) can be easily created.

10.1 SEIS-SCHOOL e-module creation process

In this section we give brief introduction to our e-module creation process, complemented by our first e-module named "The Dynamic Earth" (Boulaenko and Husebye, 2003). Figure 10.2 shows a schematic diagram depicting major tasks to be accomplished for module creation. This process is divided into two parallel running threads; the first is creation of unified content assets and the second is definition of the module structure. This two threads are coupled because available assets influence the module structure, while the logic of the module requests for certain assets. Content assets can be obtained from various sources as illustrated in Figure 10.3. The three main sources are: public domain sources, commercial sources (require permission), and home grown objects. For example, public sources might be government organizations like USGS (USA) and NASA (USA) which were major sources of content for The Dynamic Earth. Content objects like pictures, text units, animations, video clips are unified to be available for consumption by the e-module stylesheet processor. Raster pictures in numerous formats, animations and vector figures are converted using various tools to SVG format. Text units are converted to XML documents compatible with the stylesheet processor. Video clips are converted to formats compatible with MS Internet Explorer.

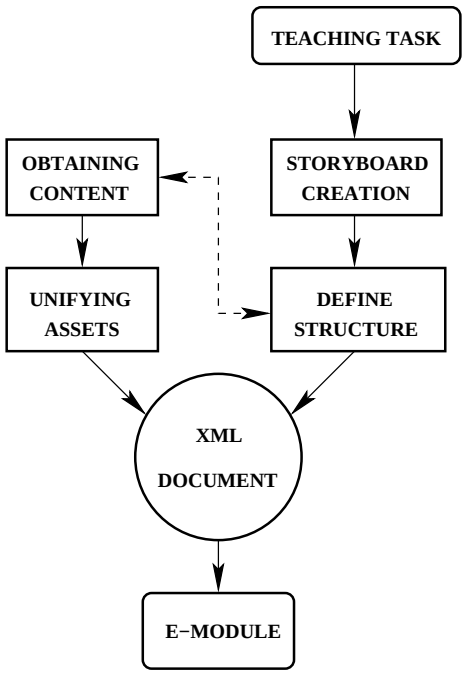

Figure 10.2: Main tasks for e-module creation.

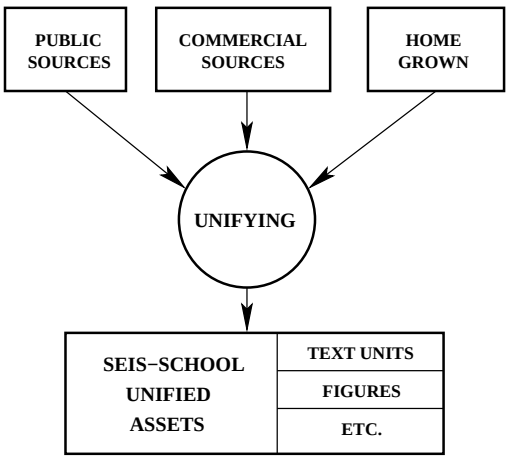

Figure 10.3: Content processing diagram.

The initial module structure is usually based of storyboard created by the responsible teacher according to the teaching task. It is being adjusted during the content collection process according to content availability. The unified assets are grouped into pages and finally the module structure is written as a XML document. A module may have hyper-structure based on hyper-links between pages.

10.2 Creating SVG animations

Animation are extremely instructive learning objects, but their use is usually limited by difficulties related to their creation. There are numerous programs available for this task most of them have unique user interfaces and thus require some special training. Simple animation are relatively easy to create, but more complex require advanced software and usually produce output in Macromedia Flash format. For the SVG format many simple tools exist while complex are still in development stage, due to relatively recent format appearance. The SVG format supports the ability for "path morphing". This is one of advanced features of modern vector animation formats and it is usually managed by complex graphics tools. It allows one to create figures which smoothly change their shape within a specified time interval. We utilize this feature in most of our animations (e.g. Pangaea, various plate boundaries).

We create our animations in a simple way avoiding the use of any commercial animation software. The creation process is depicted in Figure 10.4. Firstly we plot an initial figure in any vector editor which supports SVG format (e.g Adobe Illustrator 9.0) and store it in SVG file. Secondly, we create modified copy of the figure and define time interval needed for morphing the initial one into the modified one. During modification the number and types of control points in the paths must be preserved, as well as their symbolic labels (SVG Specification, 2001). Then repeat the second step as long as necessary. As a result we have number of SVG files which contain so-called control figures for the animation. Because SVG is actually XML document, the final work is easily done using XSL processor with appropriate stylesheet. It compiles all static SVG

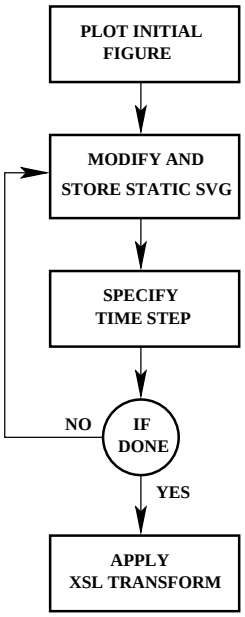

Figure 10.4: Creating SVG animations.

figures with related time steps into one SVG animation.

Chapter 11

Conclusions

The present open Web-technologies and freeware are sufficient for creation of complex e-learning modules. The compliance to high level e-learning standards such as SCORM significantly improves such issues as content reusability, accessibility, durability and interoperability. The presented design of our e-modules or Sharable Content Objects reflects a simplified form of the SCORM Learning Management System (LMS). Our design allows creation of compact stand-alone e-learning modules which can be delivered via various kinds of media (Web, CD-ROM, etc). An important advantage is excessive reuse of graphical design and programming which is otherwise provided by costly commercial authoring tools, while we manage only with open Web-standards and software.

Bibliography

[1] Advanced Distributed Learning, (2001) Sharable Content Object Reference Model, Version 1.2, The SCORM Content Aggregation Model. (www.adlnet.org)

[2] Advanced Distributed Learning, (2001) Sharable Content Object Reference Model, Version 1.2, The SCORM Overview. (www.adlnet.org)

[3] Advanced Distributed Learning, (2001) Sharable Content Object Reference Model, Version 1.2, The SCORM Run-time environment. (www.adlnet.org)

[4] Boulaenko M.E., Husebye E.S., (2003) Electronic learning modules for high school students in seismology. Seismological Research Letters. (submitted)

[5] Brogan, P., (1999) Using the Web for interactive teaching and learning. Macromedia White paper, (www.portervillecollegeonline.com/other/PDF/whitepaper_interactive.pdf)

[6] Hesthammer, J., Hesthammer, S., Johansen, S.E., and Sæther, B., (2001) Preparing for e-learning in petroleum geoscience - Part 1: Organizing, sharing and reusing content, First Break, 19, 212-217

[7] Hesthammer, J., Hesthammer, S., Johansen, S.E., and Sæther, B., (2001) Preparing for e-learning in petroleum geoscience - Part 2: Producing content, First Break, 19, 217-222

[8] Lehman Brothers, (1997) The Education Industry. (www.lehman.com)

[9] W3C, (2001), Scalable Vector Graphics (SVG) 1.0 Specification. (http://www.w3.org/TR/SVG/)

[10] W3C, (2000), Extensible Markup Language (XML) 1.0 (Second Edition). (http://www.w3.org/TR/REC-xml)

Part III

Electronic learning modules for high school students in seismology

Electronic learning modules for high school students in seismology

by

Mikhail E. Boulaenko and Eystein S. Husebye

(Submitted to Seismological Research Letters, SSA, USA)

Institute of Solid Earth Physics, University of Bergen

Allégaten 41, 5007 Bergen, Norway

December, 2002

Chapter 12

Introduction

The rapid growth and easy access to the SEIS/SCHOOL/NORWAY network (Fedorenko et al., 2000) have attracted much attention to geosciences from teachers and students alike in participating schools in Norway and also elsewhere. This has faced us with the challenge of delivering geoscience knowledge to students who stay in various locations, require stimulating learning material, and are mostly novices in a science context. The electronic learning set-up is the modern solution to this problem. The learning material is delivered in the form of E-modules - sophisticated interactive multimedia software programs (Hesthammer et al., 2001). An E-module is executed on the student's own PC-platform and provides hopefully exciting interactive learning experience. Production of a high quality module is a complex process. In order to achieve reasonable production cost, while keeping module quality high we follow a number of design principles like: i) separation of content and presentation, ii) separation of programming, graphical design, and content management, and iii) use of standard technologies. In this contribution we firstly outline E-module topics currently in production but emphasize is on technicalities in producing such modules including animations and generally availability independent of PC copyrighted software environments.

12.1 “The Dynamic Earth”

The learning module addresses the main topics related to the Dynamic Earth and the concept of Plate Tectonics, these are:

- Historical development of the plate tectonics concept
- Evidences for moving plates: continent shapes, fossils, glacier grooves, etc
- Wegener’s Continental Drift hypothesis and early objection against it
- Plate tectonics; from present to Pangaea animation over time
- The Earth’s internal structure and subdivision into plates
- Types of the plate boundaries shown in animations
- Continent collision and mountain building animation
- Paleomagnetism, and sea floor spreading magnetics
- Hot spots and whole mantle convection animation
- Global distribution of volcanoes
- Consequences of the plate tectonics

We try to add more active learning incentives by including knowledge testing via a ’Quiz’ where students are asked to answer various questions about the material given above. The main sources of figures used in displays are found on the non-profit Webpages of U. S. Geological Surveys and NASA (National Aeronautics and Space Administration). Many individual researchers have produced animations on separate modules and we did not have any problem in obtaining permission for their use in our E-module. A few videos belong to commercial companies but still no problem in obtaining permission for their use without fees. In the latter case we only used a very small part of their ’product’. The individual modules contain references to their respective sources/origins and in addition we give literature references to adequate textbooks.

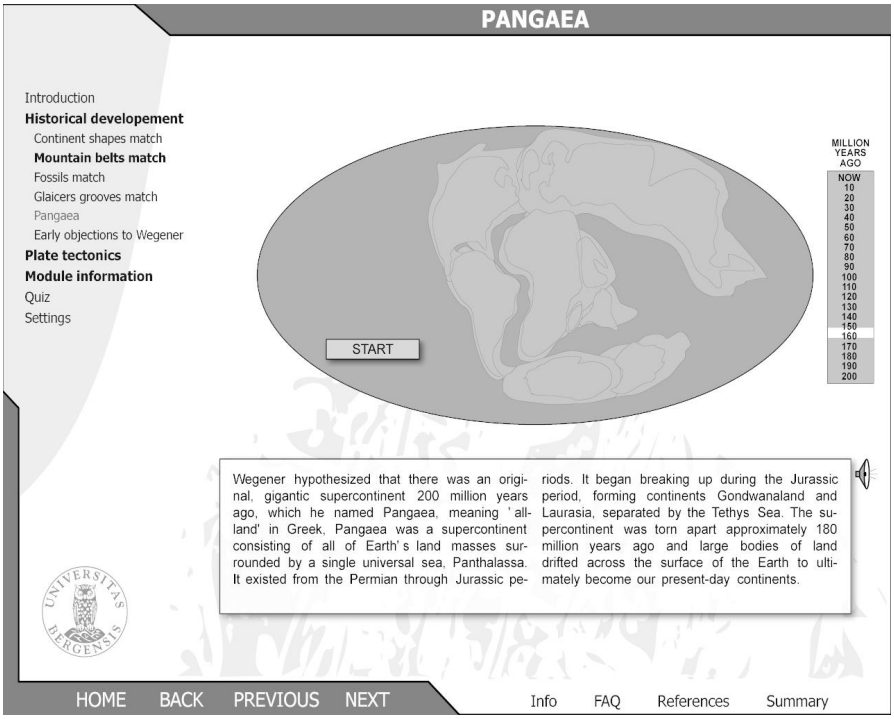

Figure 12.1: Snapshot of the Pangaea animation from the E-module "The Dynamic Earth". The animation shows continent movements since 200 million years ago until now. The relative continent position here date back 160 M.Y. (scale to the right)

12.2 "The Kinematic Earth - Its Scandinavian manifestations"

The learning module gives various geophysical information about Scandinavia, as well as detailed description of the physical processes laying behind them. Namely:

- Seismicity with time-space animation
- Tectonic map and earthquake mechanisms
- Tectonic force pattern for Scandinavia
- Free air and Boguer gravity field
- The crustal thickness and P- and S-travel times
- Earth's magnetic field and its origin and periodical reversals
- Inner core anisotropy for seismic waves
- The postglacial rebound and the principles of isostasia

The students knowledge is evaluated through limited answers quiz. The module currently in development stage and to be completed by the end of 2002.

12.3 Interactive seismogram analysis module

In the past seismogram analysis were performed by special trained analyst who seldom have any academic schooling, to read seismograms in terms of P- and S-arrival times. In the age of digital seismometry the analyst work environment has changed profoundly; recordings are displayed on a screen, phase pickings and identifications are done semiautomatically and with little extra efforts focal solutions are provided. The most advanced analysis set-ups are found at seismological data centers handling recording from all over the world like the global monitoring of the CTBTO as part of compliance monitoring of the UN comprehensive nuclear test ban treaty. We think

that such seismogram analysis abilities on the hand of high school students are essential requirement for a successful interaction with schools and are working on such an E-module. Firstly; the data base design of our SeisSchoolNorway network give students easy access to current and past earthquake recordings, several filtering options and so forth (Filatov et al. 2003). However, for this particular module we also need to provide proper background on phases appearing in the seismogram, expected travel times as a function of distance and the usefulness of polarization filtering. The ultimate goal is that of students making epicenter location and magnitude determination entirely by themselves and we so no problem in creating an analysis environment for doing so. Our work strategy here is as follow;

- Introduction; outline seismogram analysis tasks
- Earth (crust) models and travel time curve creation
- Polarization analysis; phase pickings and identification
- Single station or network preliminary event location
- Complete network data use for location
- Calculate Richter number or magnitude
- Check solutions through comparisons with past recordings
- Access Internet for open station records and general info

The above package will also require use of mapping software which schools may use in quite other context as well.

Chapter 13

General modules features

The concept of electronic learning and use of so-called E-modules in this regard is new so below we present some details on how we proceed in our E-module workings. We emphasize that since the user segment is heterogeneous high school student bodies in the context of hardware and software availability we avoid using copyrighted, costly commercial software. There are many abbreviation used so we have appendixes a list of the most commonly used expressions here. Firstly, the learning modules are build as stand-alone files of size approximately 1 - 2 Mb. The delivery format is SVG, which is described later in text. The only requirements for the student to run the module are Internet Explorer 6.0, free Adobe SVG Viewer 3.0, and free computer speech plugin. These requirements are relatively light compare to solutions based on proprietary or commercial software like Microsoft PowerPoint, etc. Our modules are provided with excessive use of interactive animations, video clips and computer generated voice descriptions. Navigation within the module is available through multilevel menus and hyperlinks. Each module's learning time is estimated to approximately 45 minutes. Module therfore are available free of charge for non-commercial use, except for a small handling and postage fee to be paid to the University of Bergen.

13.1 Design principles

Our basic module design principle was separation of content and presentation. The reason is that such an approach allows higher levels of design reuse because programming, graphical design, and content management tasks are separated from each other. At the same time they are tied by well defined and stable interfaces. The use of standard technologies for content storage and presentation significantly reduce the amount of tedious low-level work, giving us opportunity to concentrate on higher level problems. The future important challenge is compliance to SCORM (Dodds, 2001) standards and interoperability as now required in E-learning systems within the US Department of Defense (DoD).

13.2 Content

For successful segregation of learning module content we specify it as:

- number of tree structured pages and hyperlinks
- text units - text boxes (static or popup)
- figures, animations, video clips
- quiz questions and answers.

Our main requirement for the content storing format is its ability to be processed by standard management tools. Thus we do not have to spend limited resources on development of such tools and naturally ad hoc formats are not acceptable. During last years the IT society together with W3C came up with a standard way for universal data storage: XML that is a mark up language for documents containing structured information. A mark up language is a mechanism to identify structures in a document. XML is license-free, platform independent and well-supported so easy to use. For that reasons we have decided to use that format in our E-modules design. In this context

significant work has been done by Advanced Distributed Learning (ADL) initiative established by DoD, and compliance to their standards for content storage is one of our primary future challenges. Current storage format is simple and yet complex enough for current high school students teaching tasks.

13.3 Presentation format

In order to provide exiting interactive learning experience for students the presentation format must be interactive and provide high quality graphics and animations on any output device. In order to be delivered through the Internet it must be compact and for rapid module development it must also be well supported. There are number of interactive delivery formats currently in use. For example the Microsoft PowerPoint is widely used and has a steep learning curve for module producers. Main disadvantages are huge file sizes, no straight way for content/presentation separation its commercial format requires expensive software on each student's computer. Another format is the Macromedia flash, which is mainly used in interactive web graphics. Also this format is commercial and requires expensive software for module production. The Scalable Vector Graphics (SVG) format is a new XML grammar for defining vector-based 2D graphics for the Web and other applications. It was created by World Wide Web Consortium (W3C), the non-profit, industry-wide, open-standards consortium that created HTML and XML, among other important standards and vocabularies. Over twenty organizations, including Sun Microsystems, Adobe, Apple, IBM, and Kodak, have been involved in defining SVG. This is the format of our choice. The main advantages are:

- plain text format - minimum requirement for module creation is just a simple text editor
- scalable and zoomable - necessary for various learning tasks and also provides high quality graphics on any output device
- searchable and selectable text - the module can be directly searched by the Inter-

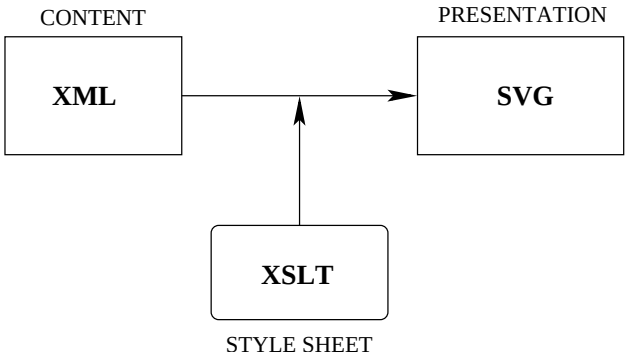

Figure 13.1: E-learning module creation process. The content is transformed into SVG graphics using an XSLT transformation document.

net search engines thus allowing wide public access

- powerful scripting and animations - vital for high quality learning material
- small file size - allows easy distribution through the Net
- Open standard, pure XML - significantly simplifies automation of E-module production process .

13.4 Automated production process

In order to create the module the final step is to compile the individual parts of design. This task is done automatically in our case. The content which is only output from the module producer is compiled with defined graphical design and software routines using a stylesheet. This stylesheet is a document which describes how to create a desired learning module from given content. It is written in XSLT (extensible Stylesheet Language Transformations) tree-oriented transformation language for transmuting instances of XML using one vocabulary into either simple text, or XML instances using any other vocabulary imaginable. We use the XSLT language to specify how to create our desired SVG output from our given structured XML input as illustrated in Figure 2.

```
<page name='Example page'>
<textbox width='5cm' y='10%'>Some text inside
the box...</textbox>
<figure y='50%' caption='Example caption for
the figure' source='figure.svg '/>
<button x='100' y='400'>Just an example
button</button>
</page>
```

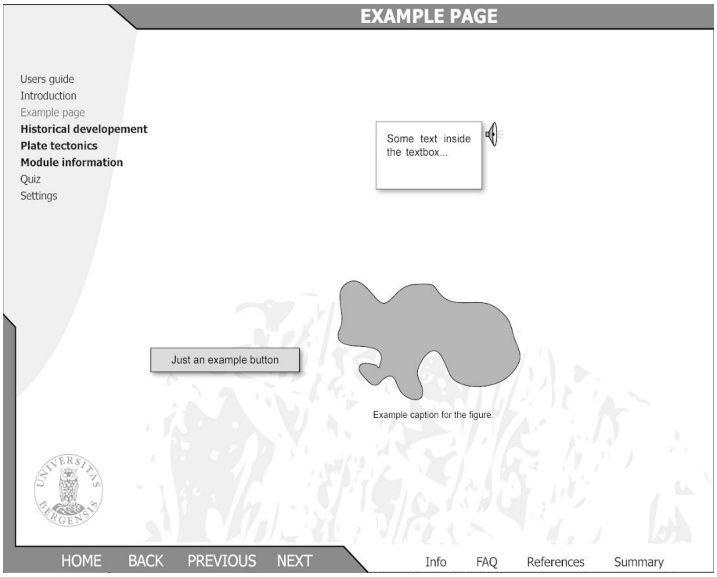

Figure 13.2: E-module page (bottom) generated from the given content (top) according to Figure 13.1.

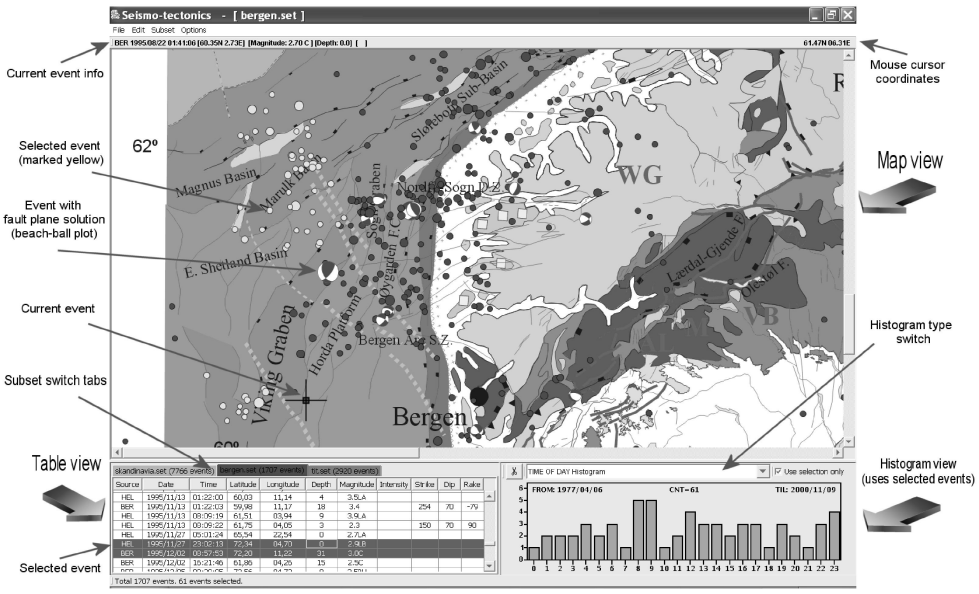

Figure 13.3: “SEISMOTECTONICS” program main window view.

13.5 Learner’s evaluation

The important part of the teaching process is evaluation of the student knowledge. Classic approach in computer based learning is quiz-like questionaries. The evaluation procedure counts student mistakes during the test. Currently we use quiz with limited number of answers as a first approximation for solving the evaluation problem. In the future we plan to add interactive schemas and maps, as well as questions which require textual answers which in turn requires manual teacher evaluations.

13.6 Practical tasks - interactive tools for statistical seismic catalog analysis

Our E-learning modules provide adequate geoscience background for interested high school students. This knowledges must alway be complemented with practical tasks simply applying the do-and-learn approach. In this framework we have developed educational quality software which allows students to perform typical analyst tasks in seismology. Our first step here is implementation of software for interactive statistical seismic catalog analysis in a Norwegian geological setting called "SEISMOTECTONICS". It allows students to analyze seismic catalogs using various histogram displays and to associate seismic activity with geological and other features like active faults, mines, road works etc. In practice we proceed in the following manner; the Fennoscandian Earthquake catalogues may contain many spurious events stemming from human activities like mining operations, industrial construction projects and so forth in addition to real earthquakes. If these false alarms are not removed before performing seismic hazard assessments, seismotectonic and seismicity studies their presence may significantly bias the final results. In extreme cases; interpreting explosion events in terms of the geological evolution of a specific area which has repeatedly happened in Fennoscandia, are destructive in a scientific context. The commonly used Fennoscandian earthquake catalogues of Ahjos et al., (1992), Uski et al., (2001), and others covering the time period 1375 - present are somewhat error prone for certain areas (W.Norway and Kola) for the interval 1970 - 2000. This time period coincide in time with deployment of many new digital seismic stations and high mining and construction activities. However, explosion activities often exhibit remarkable time distribution patterns which may be used in screening catalogues for the spurious events. The "SEISMOTECTONICS" package was developed as a part of the SEIS/SCHOOL/NORWAY project. Having user-friendly interface it can be easily operated by high-school students, albeit many analysis features are used by professionals. Based on Java technology it can be run on various computers or operating systems - Windows/Linux/Sun/Macintosh. The appli-

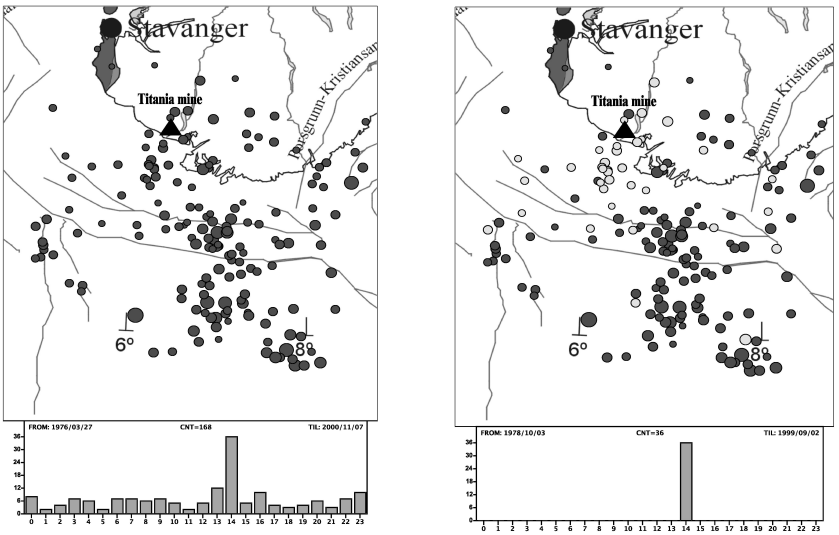

Figure 13.4: Seismic activity in SW Norway. In the left the total 168 events are plotted also in a hour-of-day histogram. To the right all 36 events occurring between 14.00-15.00 hours are marked by open circles and presumed to be explosions in the Titania mine at 14.15 +/- 5 min. These are termed spurious events also implying that location errors often exceed 10 km.

cation includes geological map of Norway (Mosar, 2000) and the mentioned Fennoscandian Earthquake Catalog covering the period 1375-2001. The software provides features for histogram and fault plane solution plotting, space-time filtering for a catalog or its subset, besides the space-time earthquake occurrence animations. The support for number of event and area subset operations like Copy/Cut/Paste/Undo/Redo/etc is included. Results of analysis - filtered catalog or its subset can be stored on disk and printed.

The program can import seismic catalog data in NORDIC and HELSINKI formats. Subsets of a catalog can be stored and retrieved in the application XML format files which are easily manipulated by large number of XML-related tools. The program currently can 'import' geological maps in JPEG, PNG, and GIF formats, but restricted to UTM projection zone 32V. The Tectonic map of Norway (Norwegian Geological Survey

(NGU) is included along with appropriate software. The map can be zoomed during analysis. A subset of events can be interactively selected from the map. Different types of histogram plots are supported: time-of-day, day-of-week, number-per-period, magnitude, and focal depth. Events which 'belong' to a certain part of the histogram can be removed from the subset, thus allowing user to perform filtering in time, magnitude, and depth domains. The map and/or histogram can be printed into SVG vector format graphics files, which can be viewed, zoomed, and printed by a Web browser with appropriate plugin, (see Adobe SVG Viewer plugin). For further editing of the images we may use vector graphical editor like Adobe Illustrator or Jasc WebDraw. The application has been tested on high-school students working with us; the student user reports were exceptionally favorable.

Chapter 14

Conclusions

Production of high quality interactive learning modules requires complex IT solutions. For academia its own E-learning module production abilities are important because they allow coupling between module design and present teaching requirements. Commercial solutions are not affordable at present due to high prices and the gap between software professionals and scientists. Separating content and presentation allows reuse of different classes of work and simplifies content production tasks. Modern well-supported technologies such as the XML-XSLT-SVG bundle provides a perfect environment for effective E-learning modules production. In the context of our Seis/School/Norway project the above E-modules now produced or being finalized are for us a perfect solution to the many request for courses to be given to both students and teachers alike. Simply, we do not have time nor money for this so these E-modules are a practical alternative to on-the-spot lectures. An added advantage is that we do not need to prepare extensive written material for the students - E-modules are self-contained in this respect. To sum up our efforts here; we have tried to utilize the teaching potential of modern multimedia software technology to communicate in a seismological manner with all participants in our School project. This also provide our clients with the possibility to apply text book knowledges in analysis of their earthquake recordings and besides testing new applications of the do-and-learn concept in the students own

environment.

Bibliography

[1] Ahjos, T., Uski, M., (1992). Earthquakes in northern Europe in 1375-1989. Tectonophysics, 207, 1-23

[2] Dodds, Ph., (2001). Sharable Content Object Reference Model: The SCORM Overview. Advanced Distributed Learning Initiative. Available at ADLNet (www.adlnet.org)

[3] Fedorenko, Yu. V., Husebye E.S., Boulaenko E.V., (2000). School Yard Seismology. Orfeus Newsletter. Vol. 2, No. 3

[4] Hesthammer, J., Hesthammer, S., Johansen, S.E. and Sæther, B., (2001) Preparing for e-learning in petroleum geoscience - Part 1: Organizing, sharing and reusing content, First Break, 4, 212-217.

[5] Hesthammer, J., Hesthammer, S., Johansen, S.E. and Sæther, B. , (2001), Preparing for e-learning in petroleum geoscience - Part 2: Producing content, First Break, 4, 217-222.

[6] Mosar, J. (2000). Depth of extensional faulting on the Mid-Norway Atlantic passive margin. Norges geologiske undersøkelse, Bulletin, 437, 33-41.

[7] Uski, M., Pelkonen, E., (2001). Earthquakes in northern Europe in 2000. Inst. Seismology, Univ. Helsinki, Report R-167

Part IV

Appendixes

Appendix A

Geophone theory

A.1 Geophone transfer function

A geophone contains a permanent magnet and a moving coil attached to a spring suspended mass. It is a simple passive electro-mechanical sensor. To obtain the ground motion from such a sensor it is necessary to know its transfer function. The sensor is considered to be a linear device, thus a simple sinusoidal signal of a given frequency on its input will be repeated at the output, but may change in amplitude. The transfer function $H(\omega)$ represents the relation between the input and output amplitudes of a simple harmonic signal as a function of frequency. Electromagnetic seismic sensors are sensitive to ground acceleration and have the voltage output proportional to the coil velocity. Their transfer function can be written as:

$$H(\omega) = \frac{G\dot{x}(\omega)}{\ddot{y}(\omega)}$$

where $\dot{x}(\omega)$ - Laplace transform of the coil velocity, $\ddot{y}(\omega)$ - Laplace transform of the ground acceleration, ω - angular frequency of a simple harmonic ground motion, G - geophone generator constant, which represents the coil voltage caused by the relative motion of the proof mass. This relation is based on the following assumptions:

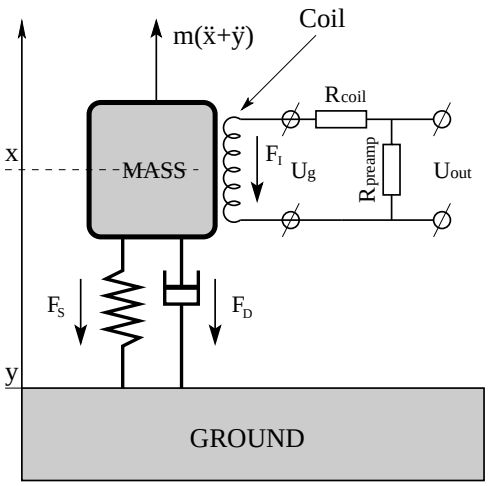

Figure A.1: Electromagnetic seismometer functional diagram.

- The geophone coil moves only in one direction, so one dimensional problem.
- The spring and the damping device are linear for all amplitude ranges of the proof mass movements.

The mathematical model of a geophone consists of several parts; a coil which also acts as a proof mass, a spring, a damping device, and a magnet connected to the ground, Figure A.1. The proof mass is connected to the ground through the spring and the damping device. When the ground is at rest the proof mass stays in the equilibrium position. When the ground accelerates the proof mass keeps its original position due to inertia. The motion of the coil relatively to the magnet generates output voltage due to changing magnetic flux inside the coil. The equation for the coil movement is described by Newton's law $\sum \mathrm{F_i} = m\ddot{x}$. Figure A.1 shows different forces acting on the coil during ground motions. The Newton's law for this system is:

$$F_S + F_D + F_I = m(\ddot{x} + \ddot{y}) \tag{A.1}$$

where F_s - spring force, F_D - damping force, F_I - force due to current induction in the coil, m - geophone proof mass, $\ddot{x}$ - coil acceleration , $\ddot{y}$ - ground acceleration. From Hook's

law the spring force is directly proportional to the coil displacement $F_s = -kx$, where k - spring constant. The damping force is directly proportional to the coil velocity $F_D = -D\dot{x}$, where D - damping constant . The force which is acting on the coil in the presence of the magnetic field is proportional to the current flowing through it, as $F_I = -I_{ind}G$ where G - geophone generator constant and I_{ind} - current inducted in the coil due to its motion. Latter can be calculated using the Ohm's law $I_{ind} = \frac{U_g}{R_{coil}+R_{preamp}}$. Where U_g - voltage generated in the coil, R_{coil} - coil resistance and R_{preamp} - preamplifier input resistance. The voltage is proportional to the coil velocity $U_g = G\dot{x}$. From above it is convenient to rewrite equation A.1 as:

$$-kx - D\dot{x} - I_{ind}G = m\ddot{x} + m\ddot{y} \tag{A.2}$$

Considering the seismograph to be a linear system, it is useful to work in the frequency domain using Laplace transform of equation A.2. So consider $x(t) = X(\omega)e^{-i\omega t}$ and $y(t) = Y(\omega)e^{-i\omega t}$ then the coil velocity will be represented as the first derivative of the coil position referred to time $\dot{x}(t) = -i\omega X(\omega)e^{-i\omega t}$ and the coil acceleration as the second derivative $\ddot{x}(t) = -\omega^2 X(\omega)e^{-i\omega t}$. The same operation is valid for the ground acceleration; $\ddot{y}(t) = -\omega^2 Y(\omega)e^{-i\omega t}$. Dropping the exponential terms rewrite equation A.2 as:

$$-kX + Di\omega X - \frac{-i\omega G^2 X}{R_{coil} + R_{preamp}} = -m\omega^2 X - m\omega^2 Y$$

then:

$$\frac{X(\omega)}{Y(\omega)} = \frac{-\omega^2}{\omega^2 - \frac{k}{m} + \frac{i\omega}{m}\left(D + \frac{G^2}{R_{coil}+R_{preamp}}\right)} \tag{A.3}$$

The last equation represents response of the spring-mass system of the sensor. It shows the same behavior as a second order high-pass filter with corner frequency:

$$\omega_0 = \sqrt{\frac{k}{m}} \tag{A.4}$$

and the damping factor:

$$h = \frac{1}{2\sqrt{km}} \left(D + \frac{G^2}{R_{coil} + R_{preamp}} \right) \tag{A.5}$$

To obtain the geophone transfer function for the ground acceleration we divide the voltage output by the second derivative of the ground motion and using equation A.3 have:

$$\begin{gathered} H(\omega) = \frac{G\dot{x}(t)}{\ddot{y}(t)} = \frac{-i\omega G X(\omega) e^{-i\omega t}}{-\omega^2 Y(\omega) e^{-i\omega t}} = \frac{iG}{\omega} \frac{X(\omega)}{Y(\omega)} = \\ = \frac{-i\omega G}{\omega^2 - \frac{k}{m} + \frac{i\omega}{m} \left(D + \frac{G^2}{R_{coil} + R_{preamp}} \right)} = \frac{-i\omega G}{\omega^2 - \omega_0^2 + 2ih\omega\omega_0} \end{gathered} \tag{A.6}$$

what is equivalent to a bandpass filter of the second order with the resonance frequency ω_0, the damping factor h, quality factor $Q = \frac{1}{2h}$, and the bandwidth $\Delta f = 2h\omega_0/2\pi \ Hz$

Only two fundamental parameters uniquely characterize the behavior of the geophone mechanical mass-spring system; the resonant frequency and the damping factor. The resonant frequency is given by the factory specification and can not be changed, while the damping factor depends on a preamplifier input resistance R_{preamp}, thus it is changeable. Latter gives opportunity to modify the geophone transfer function for various applications. Figure 2.1 shows response curves for the Geospace GS-11D 4.5Hz geophone with different damping factors applied. For high damping factors the acceleration response curve becomes flat in the frequency band around the resonance and the sensitivity decreases.

The voltage registered voltage registered by a preamplifier differs from the one generated in the coil, because the input resistance of the preamplifier is not infinite, nor the coil resistance is zero. The voltage generated in the coil U_g cause current flowing through resistors R_{coil} and R_{preamp} which represents preamplifier input resistance, Figure A.1. The preamplifier measures voltage U_{out} applied to resistor R_{preamp}, so the necessary correction for the generator constant G is:

$$G' = G \frac{R_{preamp}}{R_{coil} + R_{preamp}} \tag{A.7}$$

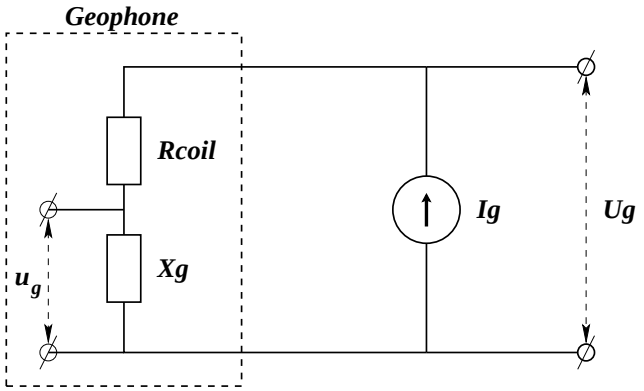

Figure A.2: Schematic diagram for the geophone impedance calculation.

The geophone sensitivity on the resonant frequency ω_0 then:

$$H(\omega_0) = \frac{-mGR_{preamp}}{D(R_{coil} + R_{preamp}) + G^2} \tag{A.8}$$

Thus depending on the geophone coil resistance as well as the preamplifier input resistance.

A.2 Geophone impedance

In order to calculate the noise level of an preamplifier it is necessary to know the geophone impedance $Z_g(\omega)$. Which can be written as $Z_g(\omega) = R_{coil} + X_g(\omega)$, where R_{coil} - coil resistance and $X_g(\omega)$ - geophone reactive resistance which changes with frequency. The reactive resistance is represented in equations as an imaginary complex number. Let assume that the ground is motionless and through the geophone connected to the preamplifier flows some external current I_g, Figure A.2. Then from Ohm's law; $R_{coil}I_g(t) + X_g(t)I_g(t) = U_g(t)$ where $U_g(t)$ - voltage generated in the geophone due to current $I_g(t)$. The geophone reactive resistance is $X_g(t) = \frac{u_g(t)}{I_g(t)}$, so $u_g(t)$ needs to be found. In order to do this rewrite equation A.1 for the geophone mass movement as:

$$F_S + F_D + F_{ext} = m\ddot{x} \tag{A.9}$$

where F_{ext} - force acting on the mass due to current I_g flowing through the coil. Rewrite it as:

$$-kx - D\dot{x} + I_{ext}G = m\ddot{x} \tag{A.10}$$

The voltage generated in the coil is $u_g(t) = \dot{x}(t)G$ and $u_g(t) = u_g(\omega)e^{-i\omega t}$, where $u_g(\omega)$ - Laplace transform of $u_g(t)$, when $\dot{x}(t) = \frac{u_g(\omega)e^{-i\omega t}}{G}$, and so $\ddot{x}(t) = \frac{-i\omega u_g(\omega)e^{-i\omega t}}{G}$ and $x(t) = \frac{u_g(\omega)e^{-i\omega t}}{-i\omega G}$ also $I_g(t) = I_g(\omega)e^{-i\omega t}$, then:

$$-k\frac{u_g}{-i\omega G} - D\frac{u_g}{G} + I_g G = m\frac{-i\omega U_g}{G}$$

and then the geophone reactive resistance is:

$$X_g(\omega) = \frac{u_g(\omega)}{I_g(\omega)} = \frac{-G^2}{\frac{k}{i\omega} - D + mi\omega}$$

The total geophone impedance is $Z_g(\omega) = R_{coil} + X_g(\omega)$. It terms of electronic components the reactive resistance can be represented by a parallel RLC contour. The contour consists of resistor, capacitor, and inductor connected in parallel. Its reactive resistance is:

$$Z_{eq}(\omega) = \frac{1}{\frac{1}{i\omega L_{eq}} + i\omega C_{eq} + \frac{1}{R_{eq}}}$$

so the equivalent electrical values for a geophone are $R_{eq} = \frac{G^2}{D}$, $L_{eq} = -\frac{G^2}{k}$, $C_{eq} = -\frac{m}{G^2}$. This values are useful for a numerical geophone modeling in electronic simulation software tools.

A.3 Summary

The formulas for the geophone transfer function and impedance were derived from its mechanical parameters. The geophone reacts as a second order bandpass filter when transforms ground acceleration to the output voltage, or as a second order high-pass

filter for the ground velocity. Slopes around the flat frequency band in the acceleration response decay proportionally to square of frequency. The quality factor Q for a geophone, which is commonly used to describe the filter behavior, is equal to $Q = \frac{1}{2h}$, where h - geophone damping factor. The geophone behavior is fully defined by three parameters: the generator constant G, the resonant frequency ω_0, and the damping factor h. Only the parameter h can be changed using different preamplifier design solutions. The damping factor depends on the coil resistance and the preamplifier input resistance. The geophone bandwidth in the acceleration domain is $\Delta f = 2hf_0\ Hz$

For any external current, flowing through the geophone coil, its reactive resistance is equivalent to the reactive resistance of a parallel RLC contour, where resistor, capacitor, and inductor are connected in parallel. Their values have been derived from the geophone mechanical parameters and its generator constant.

Appendix B

Theory of operation of the over-damping preamplifier

Then standard geophone preamplifier solutions, such as inverting and non-inverting schemas (Rodgers, 1992), are used the damping factor is limited by the coil resistance. In order to achieve stronger damping a preamplifier with the negative input resistance is required. Such preamplifier is able to provide an arbitrarily small effective damping resistance.

B.1 Design

Figure 3.2 shows the shema of the over-dumping preamplifier. The geophone is represented as an ideal voltage generator V connected in serial with resistor Z_g which represents the geophone impedance. The geophone is connected to the inverting inputs of two operational amplifiers. Both of them have the equivalent feedback networks. The negative feedback is a voltage divider build of resistor R_3 and the half of the geophone coil resistance $R_c = R_{coil}/2$. The positive feedback is a voltage divider R_1,R_2. Such a feedback configuration of two voltage dividers allows the preamplifier to provide input resistances in the range from zero to infinite, by changing values of resistors R_1,R_2

and R_3, while R_{coil} is still constant. The theory of operation of feedback amplifiers is described in Gray and Meyer (1993).

In order to analyze this preamplifier we assume that operational amplifiers are ideal and have infinite amplification, also the connection wires have zero resistance. The operational amplifiers work in the linear mode, so voltage potentials on the inverting and non-inverting inputs are equal, and the negative feedback dominates.

B.2 Transfer function

In order to find the preamplifier amplification A we refer its output voltage D to the input voltage V, then the amplification itself $A = D/V$. The output voltage is the difference between voltage potentials on the preamplifier outputs U_1 and U_2 so $D = U_1 - U_2$, (Figure 3.2). Regarding to the above assumptions we write equation for the output voltage potentials as:

$$\begin{array}{l} \frac{(U_1-0)R_2}{R_1+R_2} = \frac{(D-V)R_3}{2(R_3+R_c)} \\ \frac{(0-U_2)R_2}{R_1+R_2} = \frac{(D-V)R_3}{2(R_3+R_c)} \end{array} \tag{B.1}$$

The first equation says that the voltage difference at the resistor R_2 equal to voltage difference at the resistor R_3. The second equation says the same for the other output. Solving this equations we obtain $D = U_1 - U_2$ as:

$$D = V\frac{R_3R_1 + R_3R_2}{R_1R_3 - R_2R_c} \tag{B.2}$$

It is actually dependent on two parameters $\gamma_p = \frac{R_1}{R_2}$ - positive feedback factor and $\gamma_n = \frac{R_c}{R_3}$- negative feedback factor. So in simplified form:

$$A = \frac{D}{V} = \frac{(\gamma_p + 1)}{\gamma_p - \gamma_n} \tag{B.3}$$

If the positive feedback is eliminated $\gamma_p = 0$, the transfer function becomes $A = -\frac{R_3}{R_c}$ what is equivalent to the gain of an inverting preamplifier. If the positive feedback

factor exceeds negative, the preamplifier works in nonlinear so-called trigger mode, thus condition $\gamma_p < \gamma_n$ must be ensured.

B.3 Input resistance

In order to calculate the input resistance of the preamplifier we calculate the current flowing through the preamplifier inputs due to some input voltage V:

$$R_{in} = \frac{V}{\left(\frac{V-D}{2(R_3+R_c)}\right)} = 2R_3\left(\gamma_n - \gamma_p\right) \tag{B.4}$$

As a conclusion; to achieve the desired amplification and input resistance it is necessary to find two feedback factors γ_p and γ_n and the value of the resistor R_3. Feedback factors must satisfy the condition $\gamma_p < \gamma_n$, while values of R_3 and γ_n are depended.

B.4 Feedback resistors

According to the calculations above we find the values of the feedback resistors which will provide the desired damping and amplification. In order to do so we find the values of the positive feedback factor γ_p and the resistor R_3. Using the equations:

$$\begin{aligned} A &= \tfrac{R_3(\gamma_p+1)}{\gamma_p R_3 - R_c} \\ R_{in} &= 2R_3(\tfrac{R_c}{R_3} - \gamma_p) \end{aligned} \tag{B.5}$$

the solution is:

$$\begin{aligned} \gamma_p &= \tfrac{2R_c - R_{in}}{2R_3} \\ R_3 &= \tfrac{R_{in}(1-A)}{2} - R_c \end{aligned} \tag{B.6}$$

It is only left to find the exact values of the resistors R_1 and R_2, because only their proportion $\gamma_p = \frac{R_1}{R_2}$ affects the preamplifier parameters. Regarding to the preamplifier noise analysis given in Appendix C, values of these resistors should be as low as possible. But in order to eliminate the operational amplifier input bias current offset, the

impedances of the inverting and not inverting inputs should be equal. So according to equations C.23 and C.24 the value of the resistor $R1$ should be equal to the half of the geophone coil resistance R_c

$$\begin{aligned} R_1 &= R_c \\ R_2 &= R_c/\gamma_p \end{aligned} \tag{B.7}$$

B.5 Summary

1. The set of equations for calculation of the values for the feedback resistors $R1$, $R2$, $R3$ from a desired geophone damping factor h and preamplifier gain A, was derived.

2. In order to set a desired amplification and input resistance it is necessary to find two feedback factors γ_p and γ_n which have to satisfy condition $\gamma_p < \gamma_n$, and the value of resistor R_3.

3. The calculations can be applied to a standard inverting preamplifier by setting the positive feedback factor $\gamma_p = 0$. The positive and negative factors are equal to $\gamma_p = \frac{R_1}{R_2}$ and $\gamma_n = \frac{R_c}{R_3}$, respectively.

4. The value of the resistor R_1 is taken equal to the half of the geophone coil resistance R_c, in order to eliminate an operational amplifier input bias current offset.

5. The results are applicable for non-differential input preamplifiers, but then the value R_c has to be taken equal to the coil resistance $R_c = R_{coil}$.

Appendix C

Instrumental noise model for the over-damping preamplifier

The most common method for circuit noise calculations is to represent the noise produced by each independent element as ideal voltage and current noise sources connected externally to the circuit. This approach is described in detail by Gray and Meyer (1993). Noise level is represented in terms of root mean squares everywhere in calculations.

C.1 Preamplifier circuit equivalent noise

Because the design schematic is symmetrical the analysis can be simplified by splitting the schema into two equivalent feedback circuits. Thus calculate output noise voltage of one feedback circuit E_{fb} and then double it to obtain the total result. In mathematical terms:

$$E_{preamp}(\omega) = \sqrt{2}(E_{fb}(\omega)/A) \tag{C.1}$$

where $E_{preamp}(\omega)$ - noise voltage referred to the circuit input, A - preamplifier amplification. Then refer it to the equivalent ground acceleration:

$$N_{preamp}(\omega) = E_{preamp}(\omega)/H(\omega) \tag{C.2}$$

where N_{preamp} - preamplifier noise in units of the equivalent ground acceleration $(m/s^2)/\sqrt{Hz}$, $H(\omega)$ - geophone transfer function.

In each feedback circuit, Figure 3.2, the thermal noise of the resistors R_1, R_2 and R_3 is represented by the voltage sources u_{R1}, u_{R2} and u_{R3}, respectively, the operational amplifier current and voltage noises represented by i_{op-}, i_{op+} and u_{op}, respectively.

C.2 Thermal noise of the feedback resistors

Each resistor generates thermal noise equal to $u = \sqrt{4kTR}$. This noise is represented as an ideal voltage generator u connected in serial with a noiseless resistor R. In order to calculate the noise output caused by the thermal noise of the resistor R we need to find the difference of the output potentials $D(\omega) = U_1(\omega) - U_2(\omega)$ caused by the virtual noise source. Using the above assumption what inverting and non-inverting inputs of the operational amplifiers have the same voltage potentials we may write:

$$\begin{aligned} U_{R2} &= U_{R3} \\ U_{R2\prime} &= U_{R3\prime} \end{aligned} \tag{C.3}$$

where U_{R2}, U_{R3}, $U_{R2\prime}$, and $U_{R3\prime}$ are voltage differences on the ends of the respective resistors. Further, we apply Kirhoff's law to the whole preamplifier circuit and get a useful set of equations:

$$\begin{aligned} U_1 - 0 = (1 + \tfrac{R_2}{R_1})U_{R1} &= (1 + \tfrac{R_1}{R_2})U_{R2} \\ 0 - U_2 = (1 + \tfrac{R\prime_2}{R\prime_1})U_{R1\prime} &= (1 + \tfrac{R\prime_1}{R\prime_2})U_{R2\prime} \end{aligned} \tag{C.4}$$

Thermal noise of the resistor R_1

To obtain the preamplifier output noise caused by the thermal noise of the resistor R_1, we use equations C.3 and C.4 to write a system of equation for its noise source u_{R1}:

$$\begin{array}{c} \frac{(U_1-u_{R1})R_2}{R_1+R_2} = \frac{DR_3}{R_3+Z_g(\omega)+R\prime_3} \\ \frac{-U_2R\prime_2}{R\prime_1+R\prime_2} = \frac{DR\prime_3}{R_3+Z_g(\omega)+R\prime_3} \end{array} \tag{C.5}$$

where the noise voltage u_{R1} is added to the voltage on the resistor R_1. For simplification assume that the resistors of both operational amplifiers have the same values. Then summing the above system of equations we obtain:

$$\frac{(D-u_{R1})R_2}{R_1+R_2} = \frac{2DR_3}{2R_3+Z_g(\omega)} \tag{C.6}$$

Then the noise on the preamplifier output caused by R_1 is:

$$E_{R1}(\omega) = D(\omega) = u_{R1}(\omega)\frac{2R_2R_3+R_2Z_g(\omega)}{R_2Z_g(\omega)-2R_1R_3} \tag{C.7}$$

Thermal noise of the resistor R_2

Using equations C.3 and C.4 write a system of equations for output potentials:

$$\begin{array}{c} \frac{(U_1-u_{R2})R_2}{R_1+R_2} + u_{R2} = \frac{DR_3}{R_3+Z_g(\omega)+R\prime_3} \\ \frac{-U_2R\prime_2}{R\prime_1+R\prime_2} = \frac{DR\prime_3}{R_3+Z_g(\omega)+R\prime_3} \end{array} \tag{C.8}$$

where the noise voltage u_{R2} is added to the voltage on the resistor R_2. Then assuming that the feedback configurations are equal sum both equations:

$$\frac{(D-u_{R1})R_2}{R_1+R_2} + u_{R2} = \frac{2DR_3}{2R_3+Z_g(\omega)} \tag{C.9}$$

Then the final result is :

$$E_{R2}(\omega) = D(\omega) = u_{R2}(\omega)\frac{R_1Z_g(\omega)+2R_1R_3}{2R_1R_3-Z_g(\omega)R_2} \tag{C.10}$$

Thermal noise of the resistor R_3

Using the same assumptions for the resistor R_3 as for R_1 and R_2 have:

$$\begin{aligned} \frac{U_1 R_1}{R_1+R_2} &= \frac{(D-u_{R3})R_3}{R_3+Z_g(\omega)+R\prime_3} + u_{R3} \\ \frac{-U_2 R\prime_2}{R\prime_1+R\prime_2} &= \frac{(D-u_{R3})R\prime_3}{R_3+Z_g(\omega)+R\prime_3} \end{aligned} \tag{C.11}$$

where the noise voltage u_{R3} is added to the voltage on the resistor R_3, then summing the equations obtain:

$$\frac{DR_2}{R_1+R_2} = \frac{2(D-u_{R3})R_3}{2R_3+Z_g(\omega)} + u_{R3} \tag{C.12}$$

And finally the result is:

$$E_{R3}(\omega) = D(\omega) = u_{R3}(\omega)\frac{Z_g(\omega)(R_1+R_2)}{R_2 Z_g(\omega) - 2R_3 R_1} \tag{C.13}$$

C.3 Thermal noise of the geophone coil

The coil generates thermal noise which can be represented as a voltage source connected in serial with the geophone. For external electrical sources geophone acts as a RLC contour, which impedance has the maximum at the geophones resonant frequency. The effective input resistance of the preamplifier for a voltage source connected in serial with the coil will be:

$$P(\omega) = \frac{2R_3(R_1+R_2)}{2R_1R_3 - R_2 Z_g(\omega)} \tag{C.14}$$

where $Z_g(\omega)$ - geophone impedance. Then the noise caused by the voltage source u_{Rc} is:

$$E_{Rc}(\omega) = P(\omega) \cdot u_{Rc} \tag{C.15}$$

C.4 Noise of the operational amplifiers

Operational amplifiers generate voltage noise which is represented as an ideal voltage source connected in serial with one of the operational amplifier inputs. It can be modeled as an additional voltage difference between voltages on the resistors R_2 and

R_3:

$$U_{R2} - U_{R3} = u_{OP} \tag{C.16}$$

Rewriting equations for output potentials, we get:

$$\begin{gathered} \frac{U_1 R_1}{R_1+R_2} + u_{OP} = \frac{DR_3}{R_3+Z_g(\omega)+R\prime_3} \\ \frac{-U_2 R\prime_2}{R\prime_1+R\prime_2} = \frac{DR\prime_3}{R_3+Z_g(\omega)+R\prime_3} \end{gathered} \tag{C.17}$$

Then, assuming that the preamplifier is symmetrical write their sum as:

$$\frac{DR_2}{R_1+R_2} + u_{OP} = \frac{2DR_3}{2R_3+Z_g(\omega)} \tag{C.18}$$

Then the output voltage is:

$$E_{OPu}(\omega) = D(\omega) = u_{OP}(\omega)\frac{(R_1+R_2)(2R_3+Z_g(\omega))}{2R_3R_1 - R_2Z_g(\omega)} \tag{C.19}$$

Current noise of the operational amplifier inputs

The current noise of the operational amplifier is represented by the current sources i_{op+} and i_{op-}; see Figure 3.2. In order to calculate voltage on the preamplifier output caused by these sources we apply Kirhoff's law for the currents flowing through the nets connected to the each input. As before it is assumed that the preamplifier is symmetrical and also the assumptions for equations C.3 and C.4 are used. For the inverting input the following system of equations is adequate:

$$\begin{gathered} I_{R3\prime} = \frac{U_2 R_2}{(R_1+R_2)R_3} = I_{Zg} = \frac{-DR_1}{(R_1+R_2)Z_g(\omega)} \\ I_{R3} = \frac{U_1 R_2}{(R_1+R_2)R_3} \\ I_{R3\prime} + I_{R3} + i_{op-} = 0 \end{gathered} \tag{C.20}$$

The last equation is the Kirhoff's law for the node associated with non-inverting input of the operational amplifier. It says that the sum of all currents flowing into the node is equal to zero. The first equation tells that the current flowing through the resistor $R\prime_3$

is equal to the current flowing through the geophone, that is obvious. Then it follows that:

$$U_2 = U_1 \frac{R_1 R_3}{R_1 R_3 - R_2 Z_g(\omega)} \tag{C.21}$$

and the result is:

$$E_{OPi-}(\omega) = D(\omega) = i_{op-}(\omega) \frac{R_3(R_1 + R_2)}{R_2 Z_g(\omega) - 2R_1 R_3} Z_g(\omega) \tag{C.22}$$

which is in compressed form is:

$$E_{OPi-}(\omega) = -i_{op-}(\omega) P(\omega) Z_g(\omega)/2 \tag{C.23}$$

where $P(\omega)$ - preamplifier transfer function for an input signal caused by voltage sources connected in serial with the geophone. Using the same method for the non-inverting node obtain the noise caused by its current i_{op+} as:

$$E_{OPi+}(\omega) = D(\omega) = -i_{op+}(\omega) P_{R1}(\omega) R_1 \tag{C.24}$$

where $P_{R1} = \frac{2R_2R_3 + R_2 Z_g(\omega)}{R_2 Z_g(\omega) - 2R_1 R_3}$, that follows from C.7.

C.5 Summary

The set of equations which describes the preamplifier voltage noise spectral density on its output for each independent noise source has been developed. Because the sources are independent the total preamplifier noise referred to equivalent ground acceleration is:

$$N^2_{preamp} = \frac{2 \cdot \left(E^2_{R1} + E^2_{R2} + E^2_{R3} + E^2_{Rc} + E^2_{OPu} + E^2_{OPi-} + E^2_{OPi+}\right)^2}{(A \cdot H)^2}$$

where all E-parameters and the geophone transfer function H are frequency dependent.

1. Because the results were obtained for symmetrical differential amplifier configuration, they can also be applied for not differential amplifier design, but then $Z_g(\omega)/2$ should be replaced by $Z_g(\omega)$ everywhere in the final equations.

2. The results obtained are valid for standard non-inverting preamplifiers if the resistor $R_2 = \inf$.

3. The geophone reactive resistance affects the preamplifier noise spectra.

4. The results is applicable for preamplifiers which have frequency correction elements in their feedback networks. Then the original resistances R have to be replaced by the impedances $Z(\omega)$.

5. The total noise decreases with increasing amplification A , but the output voltage offset caused by input bias currents arise.